Abdominal Imaging

Filippo Pesapane, Marzia Acquasanta, Silvia Panella, Marcin Czarniecki, Vissaagan Gopalakrishnan, Fabio Zugni, Giovanna Gorga, Silvia Tortora, Chiara Floridi, and Gianpaolo Carrafiello

Contents

F. Pesapane (✉) · M. Acquasanta · S. Panella · F. Zugni · G. Gorga · S. Tortora
Postgraduation School in Radiodiagnostics, Università degli Studi di Milano, Milan, Italy
e-mail: filippo.pesapane@ieo.it; silvia.panella@unimi.it; fabio.zugni@unimi.it; giovanna.gorga@unimi.it; silvia.tortora@unimi.it

M. Czarniecki
Department of Radiology, MedStar Georgetown University Hospital, Washington, DC, USA

V. Gopalakrishnan
Rush Medical College, Rush University Medical Center, Chicago, IL, USA

C. Floridi
University of Ancona, Ancona, Italy

G. Carrafiello
Unità Operativa di Radiologia, Fondazione I.R.C.C.S. Cà Granda Ospedale Maggiore Policlinico, Milan, Italy
e-mail: gianpaolo.carrafiello@unimi.it

H. Amalou et al. (eds.), *The Radiology Survival Kit*,
https://doi.org/10.1007/978-3-030-84365-6_5

1 Liver

1.1 Liver Disease

Ultrasonography (US) is often a first-level instrumental investigation for the study of hepatic parenchyma with suspicion of diffuse liver disease (Table 1).

1.1.1 Hepatic Steatosis and Hemosiderosis

Although occasional, the most frequent finding in asymptomatic patients is focal or diffuse hepatic steatosis, which is an accumulation of intracellular fat. More often idiopathic than alcohol abuse, nonalcoholic fatty liver disease (NAFLD) associated with insulin resistance and dyslipidemia, acute fatty liver of pregnancy, steroid intake, and drugs can lead to hepatic steatosis [1].

Radiographic features include increased echogenicity without mass effect, and even if islands of normal hepatic tissue are present, associated with mild hepatomegaly [2].

On non-contrast computed tomography (CT), steatosis is seen as liver hypoattenuation of at least 10 HU lower than that of spleen [3] or absolute liver attenuation lower than 40 HU [4] (Fig. 1).

Table 1 Differential appearances for focal liver lesions on US and CT

	Focal liver lesion					
	Cyst	Typical hemangioma	FNH	Abscess	HCC	Metastases
US	Well-defined Thin wall Simple or lobulated Anechoic No internal vascularity on ECD	Well defined Hyperechoic Possible peripheral vessels on ECD	Difficult to detect	Poorly defined Hypoechoic No central perfusion on ECD Internal gas bubbles	Hypoechoic or inhomogeneous echotexture	Rounded and well defined Infiltrative Hypoechoic Hypoechoic halo Hyperechoic
CT	Homogeneous hypoattenuation (0–10 HU) No contrast enhancement	Hypoattenuation in non-contrast scan Peripheral enhancement on arterial phase Progressive central fill-in enhancement No washout on delayed scan	Peripheral arterial phase enhancement Isodense to liver on portal venous phase Central scar enhancement on delayed scan	Hypodense on basal scan Double target sign on contrast-enhanced CT Internal gas bubbles	Lively arterial enhancement Portal venous washout	Peripheral enhancement with possible central filling on portal venous phase and washout on delayed scan Arterial phase hyperenhancement and delayed washout Calcification or cystic component

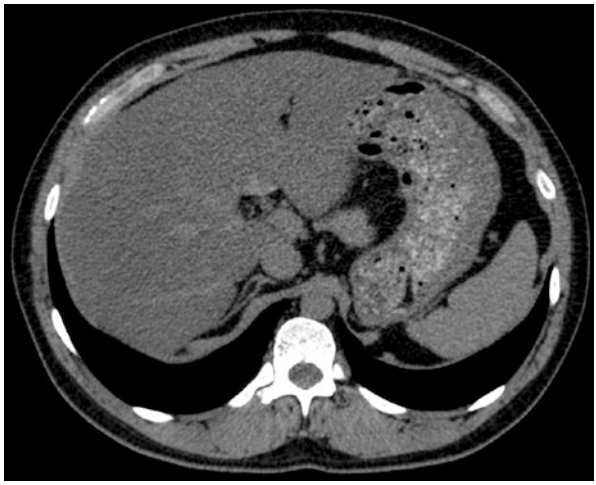

Fig. 1 Hepatic steatosis, non-contrast CT. In this patient, the liver demonstrates diffuse hypoattenuation (10 HU), compared to the spleen (50 HU)

In contrast, hyperattenuation of the hepatic parenchyma is seen in overload of hepatic iron, caused by genetic disorders, hemochromatosis, or ineffective erythropoiesis (as with repeated blood transfusions in β-thalassemia major) [5]. Magnetic resonance imaging (MRI) represents the imaging of choice for the quantification of iron; however, hemosiderosis may appear on CT as diffuse high-density liver parenchyma or high attenuating nodules [6].

1.1.2 Hepatitis

The symptoms of hepatitis are often nonspecific. The patient may present with fever, abdominal pain, and jaundice. Laboratory serum values may include an increase of hepatocellular injury levels (AST, ALT) and stasis values (ALP, GGT), plus or minus reduction of liver function (reduction of albumin and coagulation factors). The most common etiologies must be confirmed by labs and include viral infections (HAV, HCV, HBV), drug- and toxin-induced hepatitis, and autoimmune and metabolic diseases. Diagnosis of acute hepatitis remains a clinical diagnosis, even when a normal imaging appearance of the liver is present [7].

US often represents the first instrumental imaging for the suspicion of acute hepatitis. Even if it has been found to have poor sensitivity and specificity [8], a "starry sky appearance" (bright hyperechoic dots throughout hepatitis a hypoechoic liver parenchyma) is often associated with acute hepatitis [9]. Hepatitis findings include an accentuated brightness of portal vein walls, periportal edema (decreased attenuation or hypoechogenicity around the portal system and at the hepatic hilum), a diffusely low parenchymal echogenicity, diffusely low hepatitis attenuation edema on non-contrast CT, and gallbladder wall thickening. Hepatomegaly is considered the most sensitive sign of hepatitis. Hepatomegaly is defined when the liver measures greater than 15.5 cm, when measured at the midclavicular line [2].

1.1.3 Cirrhosis

Chronic liver diseases can develop into cirrhosis. Symptoms are variable depending on the degree of compensation. The clinician may suspect cirrhosis from a history of hepatic infections or biliary disease, metabolic or autoimmune disorders, vascular disease, or laboratory tests. Complications of cirrhosis include liver failure, ascites, and portal hypertension.

Even if imaging is not helpful to discover the underlying etiology, in advanced cirrhosis the liver takes on a typical morphology which involves hypertrophy of the caudate lobe and the left lobe with concomitant atrophy of the posterior segments of the right lobe. Regenerative nodules, siderotic nodules, and dysplastic nodules can be present.

US is useful for assessing surface nodularity and estimating segmental hypertrophy and atrophy [10], as well as the heterogeneous echotexture with signs of portal hypertension. As a dynamic instrument, ultrasound not only allows assessment of the caliber of the portal vein (>13 mm diameter = portal hypertension) but quantification of the portal flow (<15 cm/sec) and identification of reversed portal flow (hepatoFugal, your F'ed). By convention, doppler blue flows away from the transducer, and red is toward the transducer. Normal hepatopetal flow in the main portal vein is red (portal vein flows toward the transducer on the skin). Other findings of portal hypertension captured by ultrasound include an enlarged superior mesenteric vein and splenic vein (>10 mm), portal venous thrombosis, recanalization of paraumbilical venous flow, and portalization of hepatic vein waveform, a "corkscrew" appearance of the hepatic artery, a cluster of porta hepatis collaterals that look like a spider ("cavernous transformation" of the portal vein"). Splenomegaly and ascites may also be seen.

CT is helpful to evaluate the liver surface and parenchyma to identify regenerative nodules that are isodense to the rest of the liver, as well as siderotic nodules that are hyperdense due to accumulation of iron. In addition to assessing liver morphology and the indirect signs of portal hypertension (portal vein enlargement and portal venous thrombosis or cavernous transformation), CT allows evaluation of the liver parenchyma both on the pre- and post-contrast scans, through a dynamic study.

In this heterogeneous parenchyma, the radiologist must recognize the conditions that modify hepatic vasculature and that require an interventional procedure (e.g., TIPS - a portal to systemic shunt) and, certainly, a possible dysplastic nodule suspected for hepatocellular carcinoma (HCC or hepatoma).

1.2 Liver Focal Lesion

Focal hepatic lesions may be benign or malignant. Although some are congenital, most arise in both healthy and sick livers. Often the clinical history integrated with imaging allows good diagnostic accuracy, using the LI-RADS scale and criteria (hyperenhancement, size, rapid washout, and capsule).

1.2.1 Hepatocellular Carcinoma (*HCC)/Hepatoma*

Chronic liver diseases that evolve into cirrhosis, biliary cirrhosis, and metabolic disorders are the leading causes of HCC [11].

The symptoms are variable (constitutional symptoms, jaundice, tumor invasion of the portal vein resulting in portal hypertension, mass symptoms, tumor hemorrhage, or even upper GI bleeding varices from associated portal hypertension). The diagnosis generally is an incidental finding in the screening program for patients with risk factors. Among lab tests, alpha-fetoprotein (AFP) levels may be elevated.

On US, the small focal nodule of HCC is hypoechoic compared to normal liver, while large nodules have an inhomogeneous echotexture due to fibrosis, fat, or necrosis and calcification; a peripheral hypoechogenic halo may be present, like focal fatty sparing.

Usually, the typical HCC nodule has lively and robust arterial enhancement with subsequent washout, so it becomes iso- or hypoattenuating in the portal venous phase compared to the rest of the liver (Fig. 2). Typically, wedge-shaped perfusion anomalies may be associated. In cases of concurrent portal vein thrombosis, it is important to diagnose portal vein tumor thrombus when the thrombus itself demonstrates enhancement. "Bland thrombus" without tumor invasion of the clot does not demonstrate enhancement [12].

1.2.2 Metastases

Liver metastases are generally asymptomatic but may become symptomatic when the lesion burden compromises liver function or affects the capsule [13].

Metastases are generally rounded and well-defined and have a mass effect with distortion of neighboring vessels.

In most cases, metastases from lung cancer, breast cancer, pancreatic adenocarcinoma, and lymphoma are hypoechoic and may present with a hypoechoic halo due to fat sparing (Fig. 3).

Similarly, they are generally hypoattenuating on non-contrast CT and present with typically peripheral enhancement and sometimes with central filling on portal venous phase or washout on delayed scan. (Remember that benign hemangiomas will fill in over time from a nodular outer part to finally looking like normal liver on delayed scans.)

Metastases from melanoma, colorectal carcinoma, renal cell carcinoma, and neuroendocrine tumors are usually hyperechoic due to hypervascularization. On contrast-enhanced CT, arterial phase demonstrates corresponding hyperenhancement that later washes out on delayed phase (Fig. 4). Colorectal carcinoma metastases can have variable echogenicity on US and similarly variable attenuation and enhancement on CT, and this may change following therapies.

Calcification can occur with metastases of various mucinous adenocarcinomas, and cysts can be associated with squamous and colorectal cell carcinoma, ovarian carcinoma, and pancreatic adenocarcinoma.

On occasion, melanoma, breast cancer, and lung cancer can diffusely infiltrate the hepatic parenchyma [14].

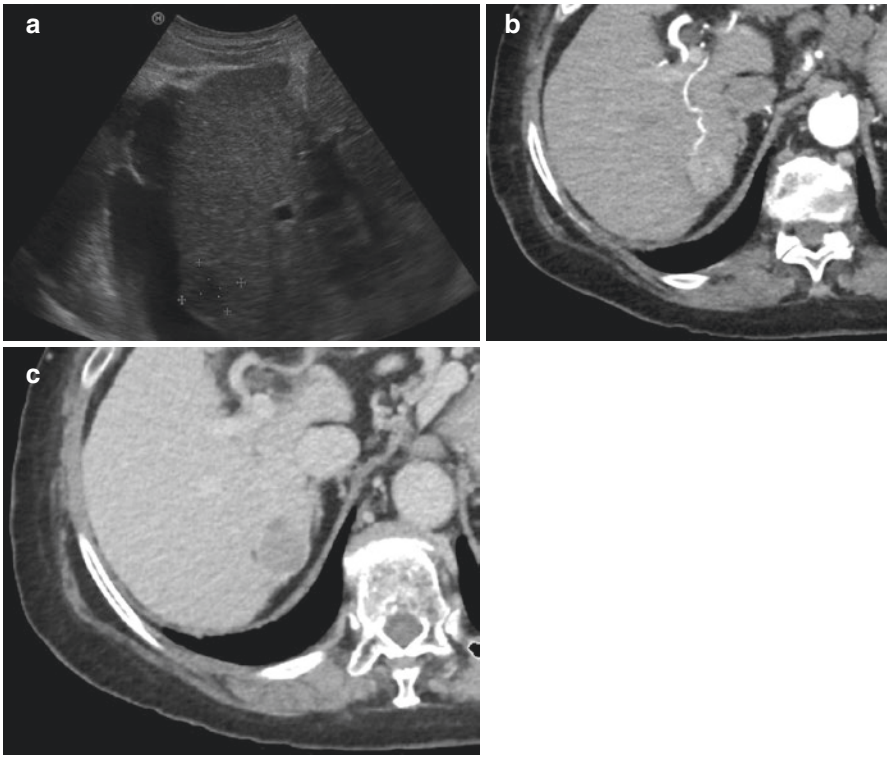

Fig. 2 HCC. US, the nodule has an inhomogeneous echotexture, hypoechoic compared to normal liver (**a**). On contrast-enhanced CT, the typical HCC nodule has lively arterial enhancement (**b**) with subsequent rapid washout, and becomes iso- or hypo-attenuating in the portal venous phase (**c**) compared to the rest of the liver. The presence of a pseudocapsule is seen (**c**). This is likely a LIRADS 4-5, which is very likely an HCC

1.2.3 Hepatic Abscess

Typically, patients with a hepatic abscess present with fever and jaundice associated with right upper quadrant pain. Other nonspecific symptoms such as anorexia, malaise, and weight loss may be seen.

Regardless of the etiology (bacterial, parasitic, or fungal), radiographic features are similar. Bacterial and fungal abscesses are often multiple, while the amebic abscesses are usually single and located in the subdiaphragmatic liver [15].

On US, hepatic abscesses are typically poorly defined with inhomogeneous predominantly hypoechoic echotexture, without central perfusion on color Doppler; gas bubbles may be seen.

On contrast-enhanced CT scan, the "double target sign" is a typical imaging feature: a central fluid-filled hypoattenuation surrounded by a hyperattenuation inner rim (that is the abscess membrane that takes early contrast enhancement which persists on delayed phase) with a hypoattenuation outer ring that is hepatic edema which enhances on delayed phase (Fig. 5). Recurrent hepatic abscesses may be

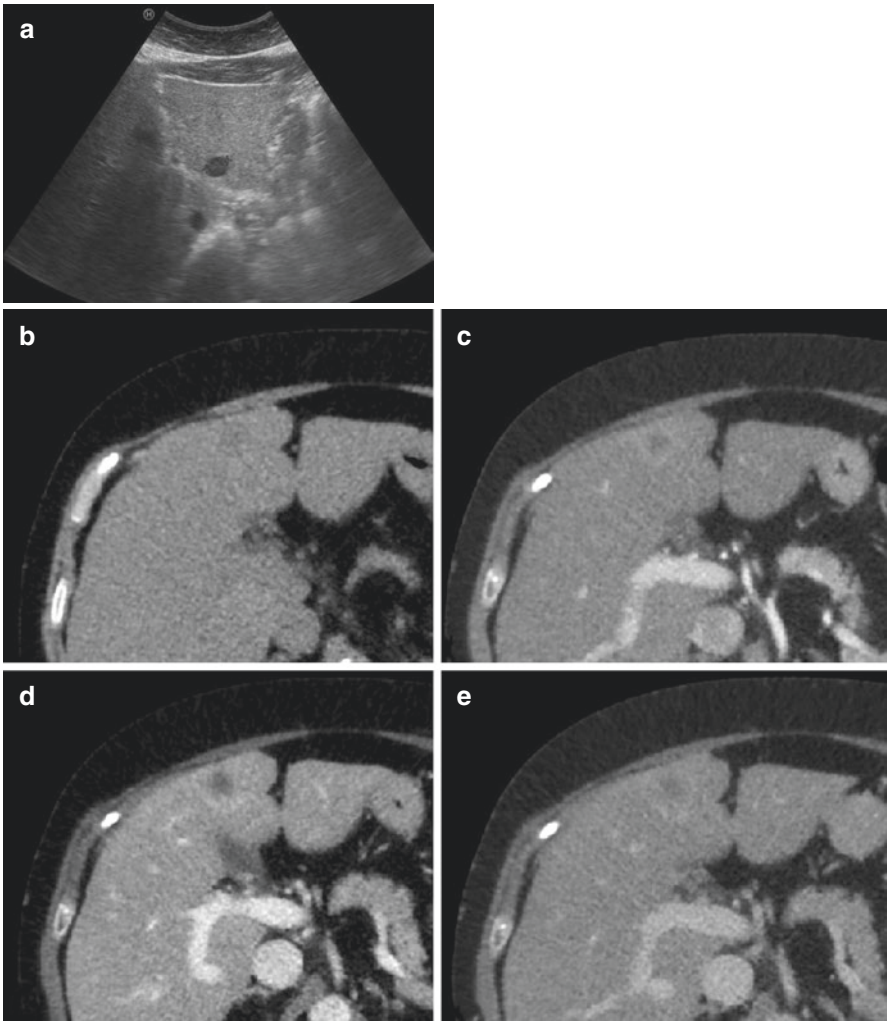

Fig. 3 Metastases from breast cancer. US (**a**), they are often defined hypoechoic lesions. On CT, metastases are generally hypoattenuating on non-contrast CT (**b**) and present typically peripheral enhancement (**c**) with possible central filling on portal venous phase (**d**) and washout on delayed scan (**e**)

associated with chronic granulomatous disease, where the white blood cells have impaired oxidative burst.

1.2.4 Other Benign Lesions: Cyst, Hemangioma, Focal Nodular Dysplasia (FNH)

Hepatic cysts are typically asymptomatic and are often incidentally discovered.

They are a round or ovoid shape with well-defined margins due to the presence of a thin wall. On US (Fig. 6), a cyst is anechoic and may be lobulated, without any

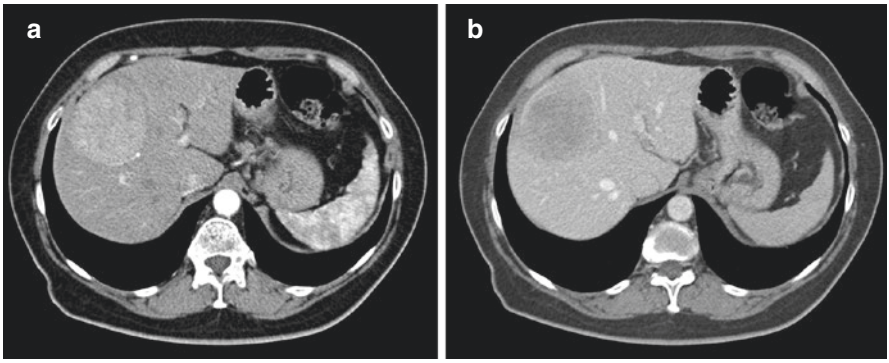

Fig. 4 Metastases from melanoma, contrast-enhanced CT. The right hepatic lobe presents a voluminous hypervascular lesion, i.e., with intense enhancement on arterial phase (**a**), which washes out on venous phase (**b**)

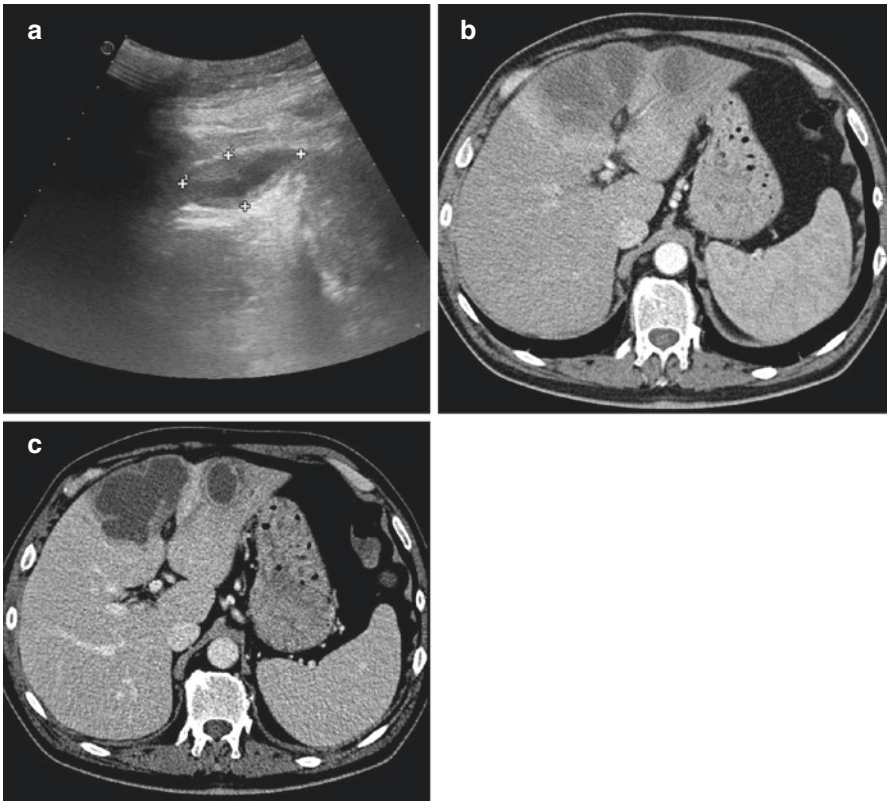

Fig. 5 Hepatic abscess. On US, the lesion has inhomogeneous and predominantly hypoechoic echotexture with corpuscular and fluid component in the context (**a**). On contrast-enhanced CT scan, the abscess presents the typical "double target sign", more evident on venous phase (**c**); an alteration of the perfusion of the neighboring parenchyma is visible on arterial phase (**b**)

Fig. 6 Hepatic cyst, US. The hepatic cyst is anechoic and has a round or ovoid shape with well-defined margins due to the presence of a thin wall. Increased "through-transmission" or sonographic enhancement is seen deep to the cyst as brighter echoes

internal vascularity on color Doppler. On CT, the cyst has a homogeneous hypoattenuation (0–10 HU) without contrast enhancement.

Benign vascular lesions of the liver may be distinctive; the most common is hepatic hemangioma. Often incidentally found, hemangiomas are well-defined hyperechoic lesions with possible peripheral vessels on color Doppler (but in a minority of cases it is hypoechoic in a relative background of diffuse hepatic steatosis). Contrast-enhanced CT is helpful to distinguish hemangioma from other malignant lesions. Typical lesions may be seen as hypoattenuating on non-contrast CT scans and demonstrate peripheral nodular-shaped enhancement on arterial phase with progressive central fill-in/enhancement on portal venous phase that does not wash out on delayed phase (Fig. 7) or becomes identical to normal liver on delayed phase.

Focal nodular hyperplasia (FNH) is generally asymptomatic and is found in young to middle-aged women who take exogenous estrogens or BCP, which may increase the size of the mass.

On US, FNH and its "central scar" are difficult to detect, while on contrast-enhanced CT, the nodule has bright arterial phase enhancement except its central scar, becomes isodense to liver on portal venous phase, and shows enhancement of the central scar on delayed phase.

1.3 Liver Traumatic Injury

In abdominal trauma, when a patient presents with right upper quadrant pain, right shoulder pain, hypotension, and shock, traumatic injury of the liver must be excluded.

Polytrauma represents a common on-call situation in which a whole-body contrast-enhanced CT is mandatory.

The radiologist must identify the presence of blood, active bleeding, and organ laceration, and the interventional radiologist may embolize for hemostasis.

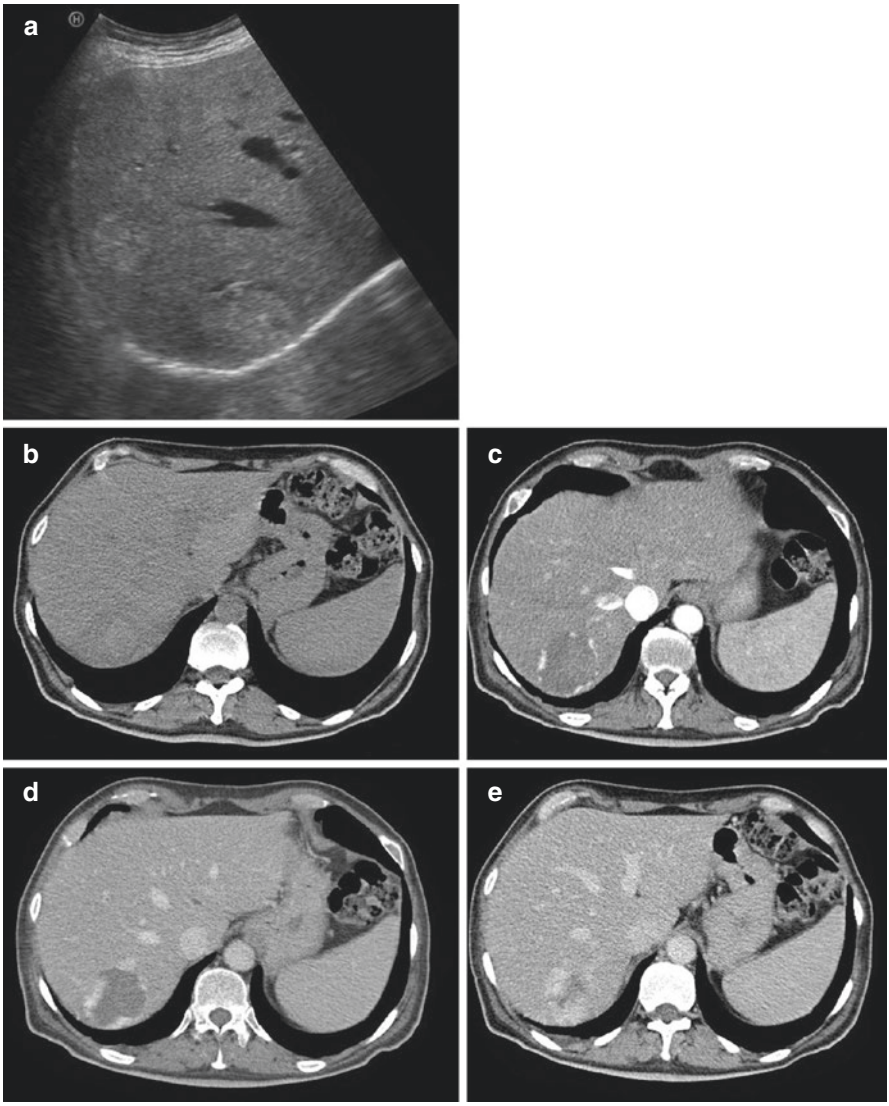

Fig. 7 Hepatic hemangioma. On US (**a**), the typical hepatic hemangioma is seen as a well-defined hyperechoic lesion. On non-contrast CT, it is seen as hypoattenuation (**b**), while on contrast-enhanced CT, it has peripheral enhancement on arterial phase (**c**) with progressive centripetal fill-in enhancement on portal venous phase (**d**) that does not readily wash out on delayed phase (**e**)

In particular, liver lacerations appear as irregular linear or branching regions of hypoattenuation. Hematomas can be subcapsular or intraparenchymal and appear as a hypodensity between the liver and its capsule extending into the hepatic parenchyma.

The acute hemorrhage is typically hyperdense (40–60 HU) compared to normal parenchyma, and the presence of blushing on dynamic phases indicates an active bleed [16] or pseudoaneurysm.

2 Gallbladder and Biliary Tract

2.1 Gallbladder Cholecystosis

Whether accumulation of cholesterol esters and triglycerides (cholesterolosis) or hyperplasia of the gallbladder wall (adenomyomatosis), US is the best test with which to assess the gallbladder.

Cholecystosis may occur as localized or, as a diffuse form, is known as "strawberry gallbladder."

Clinically silent, this condition presents like a diffuse, focal, or annular wall thickening that may be characterized by the "comet-tail" artifact, that is, the V-shaped comet tail reverberation artifact emanating from the hyperechoic adenomyoma [17].

2.2 Gallstone Disease

This condition may present as a chronic disease, in which the patient may be asymptomatic or complain of abdominal discomfort after meals with bloating. Alternatively, acute disease is characterized by pain, nausea, vomiting, and (in case of infection) fever [15].

The radiologist assesses for the presence of gallstones, correlates localized symptoms with imaging findings, and surveys for complications. The sonographic Murphy sign is a painful gallbladder upon inspiration, with the ultrasound transducer (camera) over a sensitive gallbladder below the rib cage.

In order for the gallbladder to be bile-filled, therefore assessable, the patient must be fasting.

Some radiopaque gallstones may be seen on the plain radiograph (Fig. 8a), but ultrasound is the best single initial test for seeing gallstones and their complications [18], although a nuclear medicine HIDA scan can be used to diagnose a blocked common bile duct.

Regardless of their composition, gallstones are hyperechoic structures that move according to gravity with the patient position changes (the rolling stone sign), characterized by prominent posterior acoustic shadowing. On color Doppler, the stone may demonstrate the twinkling artifact, a focus of posterior alternating colors which simulates turbulent blood flow [18].

When the gallstone is wedged in the common bile duct (choledocholithiasis), a dilatation of the biliary tree upstream plumbing is seen (Fig. 8b).

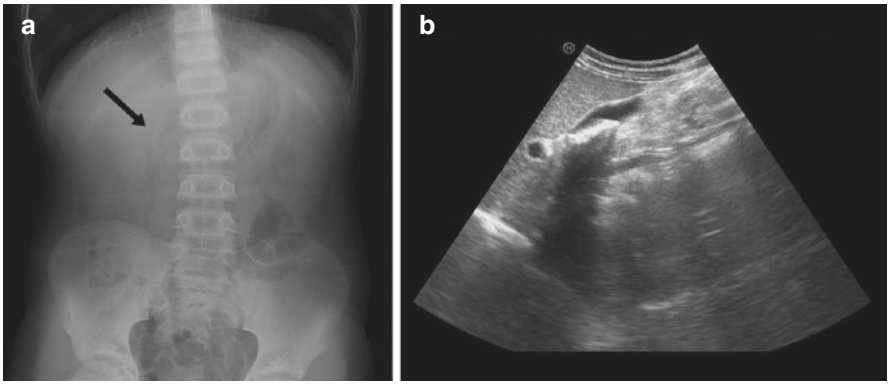

Fig. 8 Gallstone disease. On the plain radiograph (**a**), many small radiopaque densities are projected adjacent to the right lumbar spine (black arrow). On US (**b**), gallstones are seen as hyperechoic structures; prominent posterior acoustic shadowing is present

Depending on their composition on CT, gallstones may be hypoattenuating to bile (pure cholesterol stones), hyperattenuating (calcified gallstones), or isodense to bile. The latter are not clearly identified on CT [19] but might be easier seen on MRCP.

Acute cholecystitis as complication of cholelithiasis is characterized by intermittent right upper quadrant pain of biliary colic, and gallstone obstruction is often in the gallbladder neck or in the cystic duct. A minority of cases of cholecystitis are acalculous (ICU, burns, or vasculopathy). In addition to sonographic evaluation of the gallstone and gallbladder distention, the US demonstrates the presence of acute cholecystitis when gallbladder wall thickening (>3 mm) and pericholecystic fluid are seen.

The same findings can be seen on CT scan, which can also demonstrate mural or mucosal gallbladder hyperenhancement and possible enhancement of the adjacent liver parenchyma, even if stones isodense to bile are usually missed [20].

Although rare, emphysematous and suppurative cholecystitis must be excluded because they represent a potential surgical emergency. A boards question associates *E. coli* in diabetics with emphysematous cholecystitis (gas in gallbladder wall).

In the first case, the radiologist may see the gallbladder wall necrosis through the presence of gas in the lumen or wall, best detected on contrast-enhanced CT [21]. A possible perforation is demonstrated by the presence of pneumoperitoneum.

In the suppurative cholecystitis, the sonographic and densitometric findings are identical to cholecystitis with the exception of hyperechoic/hyperattenuating content often seen within the gallbladder lumen [20]. Another boards question might associate acalculous cholecystitis (no stones but dilated gallbladder or hydropic gallbladder and gallbladder wall thickening) in a patient who is a vasculopath, in ICU, burn unit, or posttrauma. The treatment is a cholecystostomy tube (gallbladder tube) placed at the bedside by IR.

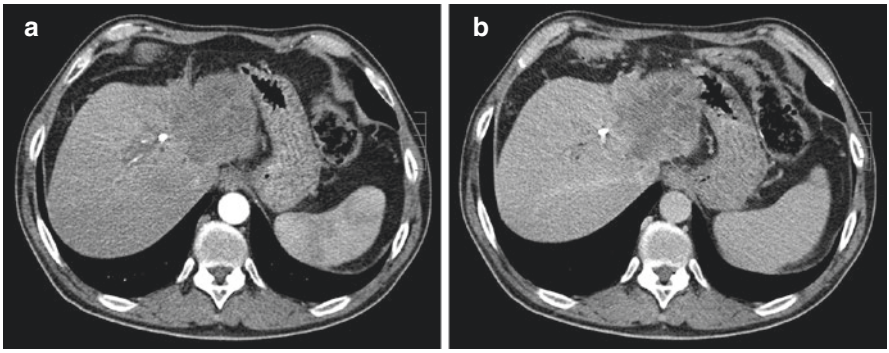

Fig. 9 Mass-forming cholangiocarcinoma, CT. The tumor demonstrates minor peripheral enhancement (**a**) with gradual centripetal enhancement (**b**) which depends on the degree of central fibrosis

2.3 Cholangiocarcinoma

Often the only clinical presentation of cholangiocarcinoma is insidious jaundice, the primary reason the patient undergoes investigations. Even if MRI is the imaging modality of choice, it is important to suspect a cholangiocarcinoma to direct the patient toward the correct diagnostic procedure.

Cholangiocarcinoma is often extrahepatic and, less often, intrahepatic, in the mass-forming, periductal infiltrating, or intraductal variant. It is usually central near the porta hepatis.

The mass-forming tumor variant presents as a homogeneous isoechoic mass with a hypoechoic periphery; capsular retraction may be present. On CT, it demonstrates minor peripheral enhancement with gradual centripetal enhancement which depends on the degree of central fibrosis (Fig. 9).

Periductal infiltrating and intraductal tumors are characterized by altered caliber bile duct, typically at the hepatic hilum, with peripheral dilation of the biliary tree, without the presence of a well-defined mass. When seen, the polypoid mass is usually hyperechoic in the intraductal tumor and demonstrates contrast enhancement on CT [22].

3 Spleen

Most primitive splenic lesions are detected incidentally. Conventional ultrasonography allows confident detection of cystic lesions but is less accurate for characterizing lesions with solid components, which should be evaluated with contrast-enhanced CT. Contrast-enhanced ultrasonography (CEUS) may be an optimal alternative to CT, when available [23].

3.1 Cysts

Splenic cysts can be either congenital (true cysts) or acquired (secondary/false cysts or pseudocysts). These may be indistinguishable on imaging.

Congenital cysts may be multiple or isolated and present as intraparenchymal, unilocular fluid-filled structures with thin epithelial walls, hypoattenuating on CT without contrast enhancement. Congenital desmoid cyst is an exception since it may show a thickened wall with linear enhancement. Splenic lymphangioma is a relatively rare congenital malformation of lymphatic ducts and usually appears as a complex multiloculated cyst with septa. It is usually subcapsular and does not enhance after contrast, although fine internal vessels may be seen [24, 25]. All the congenital cysts may be complicated by superinfection (visible as solid intralesional debris and calcification) or hemorrhage (fluid-fluid levels and hyperattenuation on CT) [24].

Secondary cysts occur after traumatic splenic injury or infection and are more common than simple congenital cysts. These appear as fluid collections with no epithelial lining and possible mural calcifications [23]. Splenic parasitic echinococcal cysts (hydatid cysts) are rare infective cysts with a complex structure characterized by septa and wall calcifications; their complexity is related to the stage of the infection [23, 25].

3.2 Hemangioma

On ultrasound, splenic hemangiomas are hyperechoic with irregular but defined margins. CT typically shows an irregular enhancing pattern (unlike hemangiomas in the liver) which is usually nodular and peripheral and may progress heterogeneously during the venous and late phases. Cavernous variants show internal cystic areas and often incomplete enhancement due to thrombosis and/or fibrosis [23].

3.3 Hamartoma

Hamartoma is a benign malformation originating from the red pulp, containing disorganized vascular channels in a fibrous stroma. On ultrasonography, it presents as an inhomogeneous hypoechoic structure, with internal anechoic foci and septations, and hypervascularity on color Doppler. On CT, hamartomas are usually isoattenuating compared to splenic parenchyma, with fatty components and internal calcifications, which may be hardly detectable after contrast administration. Multiphase contrast evaluation shows centripetal or centrifugal enhancement progression and may be difficult to distinguish from a splenic hemangioma [23].

3.4 Abscess

Splenic abscess is an uncommon finding, which usually presents as a complication of a penetrating injury or during infectious or septic conditions, such as endocarditis often related to intravenous drug abuse. Suggestive symptoms and findings include fever, left upper quadrant pain, and leukocytosis. In the suspicion of abscess, ultrasonography-guided drainage is required as the first step of therapeutic management. Different patterns are observed according to the underlying pathogen [24]. Septic emboli are wedge-shaped triangles, with the base along the capsule.

3.4.1 Pyogenic Abscess

On ultrasonography, a pyogenic abscess presents as an isolated hypoechoic lesion with irregular wall. When large (2–3 cm) it may show an anechoic core with septa or reverberation artifacts due to gas bubbles. On CT, findings suggestive for an abscess include a focal area with irregular margins and hypoattenuation reflecting the presence of necrosis or possibly containing gas bubbles. Enhancement may be present in large, encapsulated, or organized abscesses and involve the external margin (ring enhancement) and internal septations. Late contrast washout is usually seen. Wedge-shaped regions of low attenuation and reduced vascularization in the surrounding parenchyma indicate subsequent infarctions, often due to septic emboli [24]. Septic emboli and resulting ischemia may appear as triangular lesions with broadly based at the outer capsule, especially in organs with one blood supply (spleen, brain, kidney, lung). For example, in the lung a pulmonary thromboembolus may produce a "Hampton's hump," which is a wedge-shaped area of lung infarction.

3.5 Fungal or Parasitic Abscess

Fungal and parasitic splenic abscesses present usually as multiple lesions, less than 2 cm in size. On ultrasound, they show a hypoechoic structure with a target-like or "wheel within a wheel" morphology. Usual pathogens associated with this pattern are fungi and *Pneumocystis carinii*, mostly observed in immunocompromised patients.

3.6 Mycobacterial Abscess

Mycobacterial abscesses present as multiple small lesions of 10–20 mm in size with a hypoechoic structure [25]. Mycobacterial lymph nodes can have low attenuation (dark).

3.7 Infarction

Splenic infarction (SI) is either caused by occlusion of the splenic artery, venous thrombosis of the sinusoids, or by arterial embolism. Other possible causes include

pancreatic diseases and portal hypertension, leading to thrombosis of the splenic vein [24]. Isolated gastric varices may suggest splenic vein thrombosis, based on vascular plumbing.

Ultrasonography is not useful in the acute phase, with false negatives rising up to 50% of cases. When evident, SI are displayed as hypoechoic triangular lesions. Organ swelling may occur due to the development of edema. Color Doppler may reveal acute splenic infarcts, especially if large, as an area of reduced vascularity compared to the normal parenchyma. If available, CEUS drastically improves the detection of SI. In the late healing phase (due to fibrosis or scarring), the infarctions become more evident and become hyperechoic [25].

CT shows a higher sensitivity for SI, especially in the acute phase. The infarcted area is seen as triangular reduced attenuation with indistinct margins; the base of the triangle is always directed toward the splenic capsule (Fig. 10). Organ swelling may

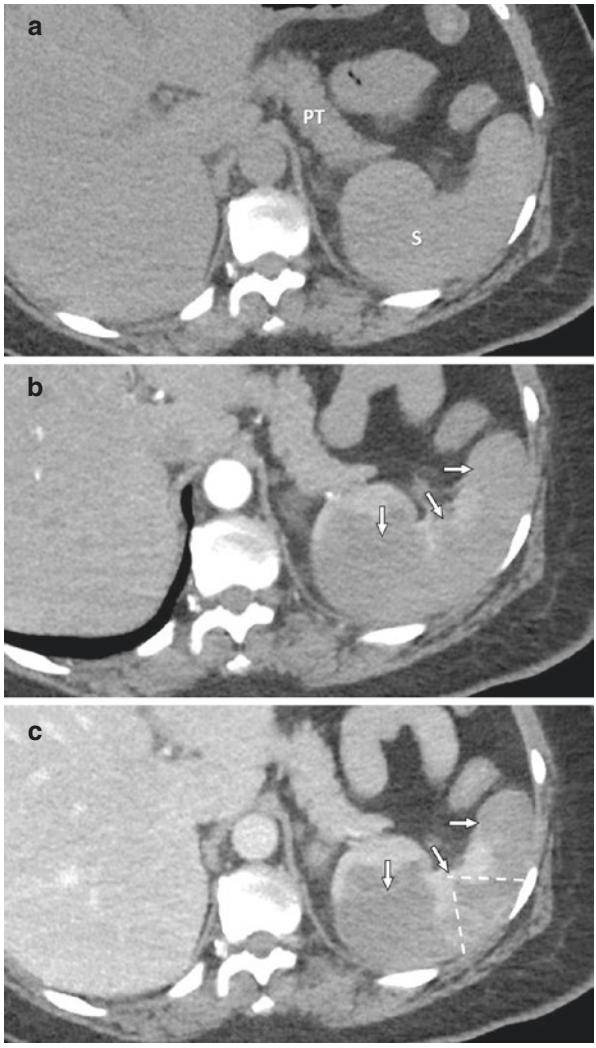

Fig. 10 Infarction of the spleen, CT. Contrast-enhanced CT scan performed in a 55 year old woman after an episode of arterial embolism caused by atrial fibrillation. Images acquired before contrast media injection (Fig. a) show no abnormality. Images acquired during arterial phase (Fig. b) and venous phase (Fig. c) reveal multiple large infarctions in the spleen (arrows) which show no enhancement when compared to pre-contrast images. The infarcted areas show a vaguely triangular shape, with the base of the triangle coinciding with the splenic capsule (dotted lines in Fig. c). Abbreviations: pancreatic tail (PT), spleen (S)

also be evident. After contrast administration, CT reveals characteristic triangular areas of reduced perfusion. In the subacute phase, the lesions experience volume loss due to necrosis, associated with further reduced attenuation. By the late phase, infarcts evolve into areas of fibrosis with bright calcifications [16, 23–25].

4 Pancreas

4.1 Acute Pancreatitis

Diagnosis is obtained when at least two of the following criteria are satisfied: [1] abdominal pain, [2] amylase/lipase >3 times the upper normal value, and [3] characteristic imaging findings. Since severity might be underestimated in the early phase disease, it is best to perform a second assessment at imaging in the advanced phase (from the second week since onset of symptoms), in order to optimize treatment and identify complications (Fig. 11) [26].

Ultrasonography has no role in acute diagnosis but may be performed for detecting stones or biliary dilatation and for monitoring fluid collections.

CT should be performed roughly 72 h after the onset of symptoms. Indications for CT include the confirmation of diagnosis, the evaluation of clinically severe AP, reassessment due to lack of improvement following initial treatment, assessment for pseudocyst, or ruling out pancreatic adenocarcinoma as an underlying cause of AP in patients >40 years of age [27]. If complications are not present at the first imaging (72 h), a reevaluation in the late phase is recommended.

Two types of AP include interstitial edematous pancreatitis (IEP) and necrotizing pancreatitis (NP).

4.1.1 Interstitial Edematous Pancreatitis

Focal or diffuse enlargement without necrosis and mild peripancreatic fat stranding due to fluid [26]. Complications of IEP include:

- Acute peripancreatic fluid collection: <4 weeks since onset of AP, fluid collections surrounding the pancreas, no discreet walls, spontaneous resolution.
- Pseudocyst: ≥ 4–6 weeks, fluid collection confined within a wall, possible communication with main pancreatic duct (MPD), spontaneous resolution. Takes 4–6 weeks to develop and organize. Endoscopic ultrasound can also drain into the stomach.

4.1.2 Necrotizing Pancreatitis

Areas of low density and reduced enhancement in ≥30% of the gland indicating necrosis (Fig. 12) [26]. Complications of NP include:

- Acute necrotic collection: <4 weeks, dense fluid collections (necrotic debris) within or near the gland, possible communication with MPD.

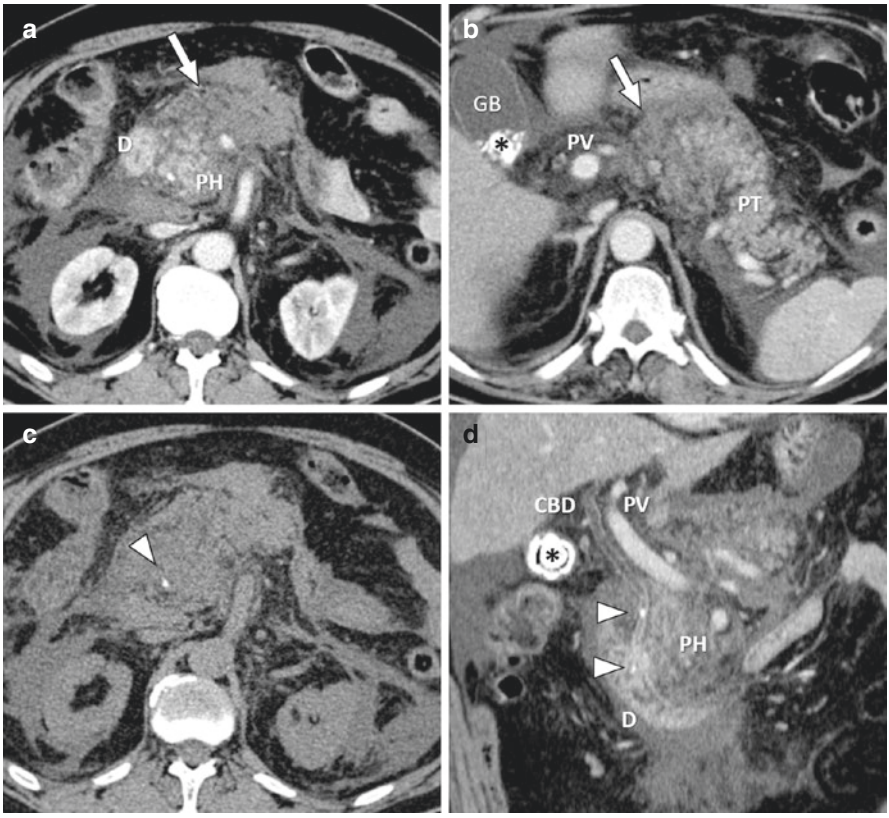

Fig. 11 Acute pancreatitis in early phase, CT. Contrast-enhanced CT obtained in a 53 year old man for confirmation of acute pancreatitis at the time of admission. Figures a and b obtained after intravenous contrast administration show possible initial necrosis in the pancreatic body (arrow) seen as a faint area of reduced enhancement, compared to the normal parenchyma of the head and tail of the gland. Acute peripancreatic fluid collections (APFC) can be seen surrounding the pancreas and in the intraperitoneal space anterior to the kidneys. Figure c acquired before contrast administration shows a focal hyperattenuating object in the pancreatic head, representing a calculus (arrowhead) causing biliary obstruction and pancreatitis. A coronal reformation in Fig. d shows actually two calculi causing obstruction of the common bile duct (arrowheads) and a larger one in the gallbladder (asterisk in figures b and d). Abbreviations: duodenum (D), portal vein (PV), pancreatic head (PH), pancreatic tail (PT), common bile duct (CBD)

- Walled-off necrosis: ≥4 weeks, collection of non-fluid debris within a thickened wall of granulation tissue, requires surgical resection. This is similar to infected solid tumors that may also be difficult to treat with small IR tube drainage, due to solid phlegmonous material or solid tumor debris.

Necrotic collections may develop superimposed infection as a further complication. This is usually evident from the presence of free extraluminal gas in the

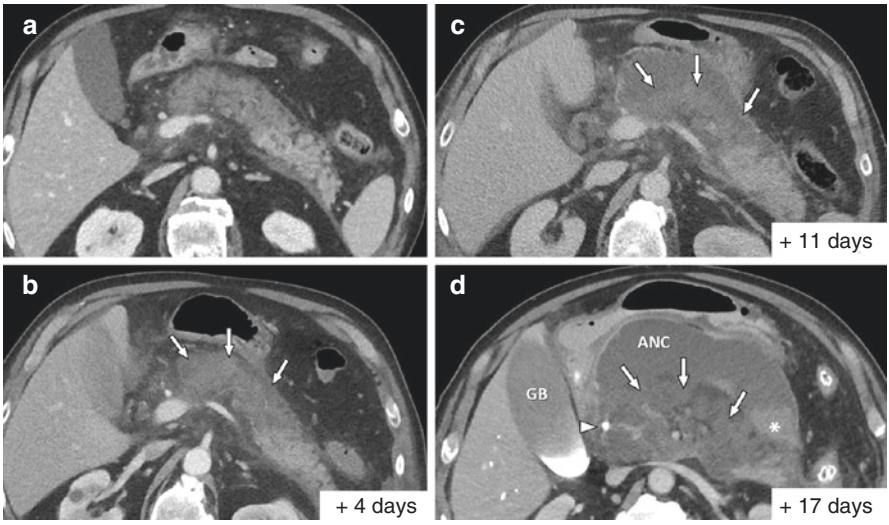

Fig. 12 Development of acute necrotic collection in necrotizing pancreatitis, CT. Contrast-enhanced CT scan was performed for the characterization of early acute, revealing a faint area of reduced enhancement in the pancreas as seen in Fig. a. A second CT performed four days later (Fig. b) clearly shows further increase in the hypoattenuating area in the pancreatic body, strongly suggestive for necrosis (arrows). Two other CT scans performed respectively 11 and 17 days after the first (Fig. c and d) show persistence of the necrotic area (arrows) and progressive development of a fluid collection anterior to the pancreas. Figure d shows a large acute necrotic collection (ANC) with a dense anterior wall and fluid-debris level (asterisk). Due to mass effect on the common biliary duct causing biliary obstruction and icterus, percutaneous drainage of the common bile duct was performed, resulting in the collection of hyperattenuating contrast media in the duct (arrowhead) and in the gallbladder (GB)

abdomen. Other possible signs consistent with necrosis are air bubbles or gas-fluid levels in the collection [27].

Reassessment should be performed if the clinical picture suggests complication, in cases of severe AP (7–10 days after admission and before discharge) and to assess efficacy of surgical treatment. All that is dark on CT may not be fluid. Ultrasound is the best method to tell solid from cystic. High interstitial pressures in tumors can also preclude enhancement and look like necrosis.

4.1.3 Chronic Pancreatitis

Imaging is utilized to diagnose chronic pancreatitis and to grade its severity. Early CP should be evaluated with MRI +/− MRCP, as CT shows low sensitivity. In late CP, typical CT findings include dilation of the main pancreatic duct (MPD) and side branches, with irregular contour of the ducts. Parenchymal atrophy may be present, although not specific for CP, as atrophy (with fatty replacement) is common and normal in older ages. Parenchymal or intraductal calcification may be seen in those cases of CP that are related to alcohol use. Occasionally, enlargement of the pancreatic head may mimic tumor [27].

Complications include pseudocyst, pseudoaneurysm, splenic vein thrombosis, and compression on biliary ducts due to mass effect.

4.2 Cystic Pancreatic Lesions

Most common lesions in this category include *intrapancreatic mucinous tumors (IPMN), mucinous cystic neoplasms (MCN), serous cystic adenoma (SCA), and pseudocysts* [28] (Table 2).

Ultrasonography may be used as a surveillance tool but not for diagnosis.

CT detects malignant features when present, although correct classification is not always possible. Fig. 13 shows a main duct IPMN on contrast-enhanced CT.

Small, unilocular, and asymptomatic pancreatic cystic lesions for which classification is not possible should be reassessed at 6 and 12 months after detection [27, 28]

4.3 Pancreatic Adenocarcinoma (PDA)

Ultrasonography has very low accuracy for the detection of PDA, and its use is limited to assessment for concomitant biliary obstruction or choledocholithiasis. Due to overlying bowel gas, the pancreas may be hard to visualize on US.

Contrast-enhanced CT with arterial and venous phases, multi-planar reconstruction and super thin slices is required for staging. Contrast is mandatory for detection, as PDA is usually hypovascular compared to the normal gland. Typical signs include mass effect with interruption and dilation of the MPD and of the common bile duct, as well as atrophy of the distal parenchyma (Figs. 14 and 15). CT shows moderate sensitivity for hepatic and regional lymph node metastases [27].

Local staging is performed with either contrast-enhanced CT or MRI. The National Comprehensive Cancer Network guidelines for local staging classify tumors as either resectable, borderline resectable, or unresectable, with regard to the possibility of a curative resection with disease-negative margins. Resectability

Table 2 Pancreatic lesions

Lesion type	Sex, age, site	Characteristic CT findings	Malignant features
SCA	F 75%, M 25% 60–70y Head, body, tail	Microcystic (<2 cm) Sponge-like, lobulated Calcifications (central) Central scar in 1/3 No communication with MPD	None (usually *benign*)
IPMN side branch	F 40%, M 60% 60–70y Head, body, tail	Macrocystic “Bunch of grapes” shape Communicates with MPD	>6 mm MPD dilation Size >3 cm Mural nodules (*Surveillance possible*)
IPMN main duct	F 40%, M 60% 60–70y Head, body, tail	Diffuse MPD duct dilatation	>10 mm MPD dilatation Mural nodules (*Resection recommended*)
MCN	F 40–50y Body, tail	Macrocystic Oval with thick walls Calcifications (peripheral) No communication with MPD	Solid component Peripheral calcification (*Resection advised*)

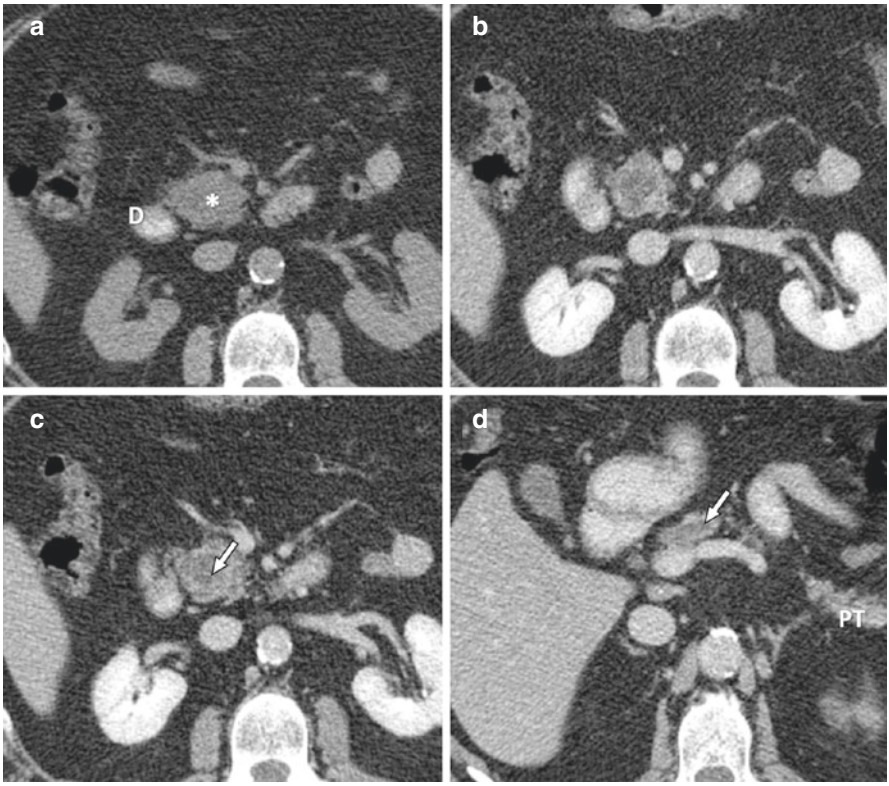

Fig. 13 Main duct IPMN, CT. Contrast-enhanced CT of a 70 year old man show a hypodense cystic lesion in the pancreatic head of fluid density (asterisk in **a**) without significant enhancement compared to the surrounding parenchyma after contrast enhancement (**b**. The lesion measures 22 mm suggestive for macrocystic type and shows growth inside the main pancreatic duct (arrow in **c** and **d**). Location, MPD involvement and macrocystic features suggest main duct intrapapillary mucinous neoplasia (IPMN) as the most likely diagnosis. Abbreviations: duodenum (**d**), pancreatic tail (PT)

criteria are based upon the involvement of nearby arteries (superior mesenteric artery, common hepatic artery, celiac trunk) and veins (superior mesenteric vein, portal vein) [29].

Distant staging must be performed once the patient has been classified as having a resectable or borderline resectable PDA. A contrast-enhanced MRI of the liver and a contrast-enhanced CT of the chest are then required to evaluate for distant metastases [29].

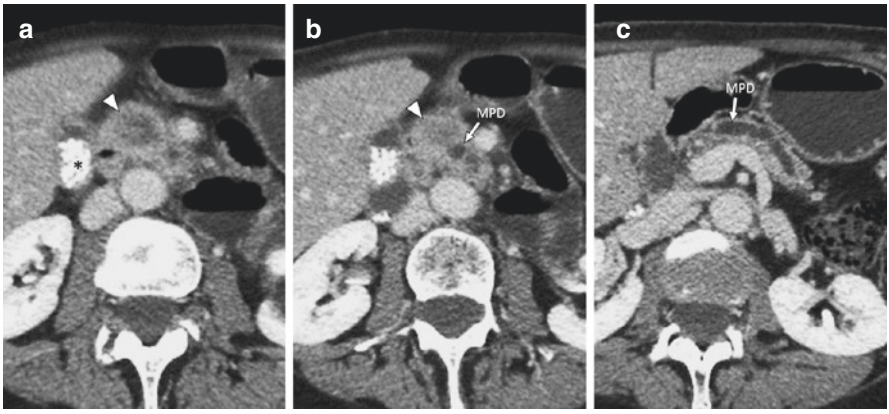

Fig. 14 Pancreatic adenocarcinoma, CT. Contrast-enhanced CT performed in a 62 year old woman shows a 30 mm lesion located in the pancreatic head with indistinct margins (arrowhead in **a**) and reduced enhancement compared to normal parenchyma, . The lesion's size causes mass effect on surrounding structures, with retro-dilation of the main pancreatic duct (arrow in **b** and **c**). The parenchyma of the pancreatic tail shows moderate atrophy. Innumerable hyperattenuating biliary stones can be seen in the gallbladder (asterisk in **a**)

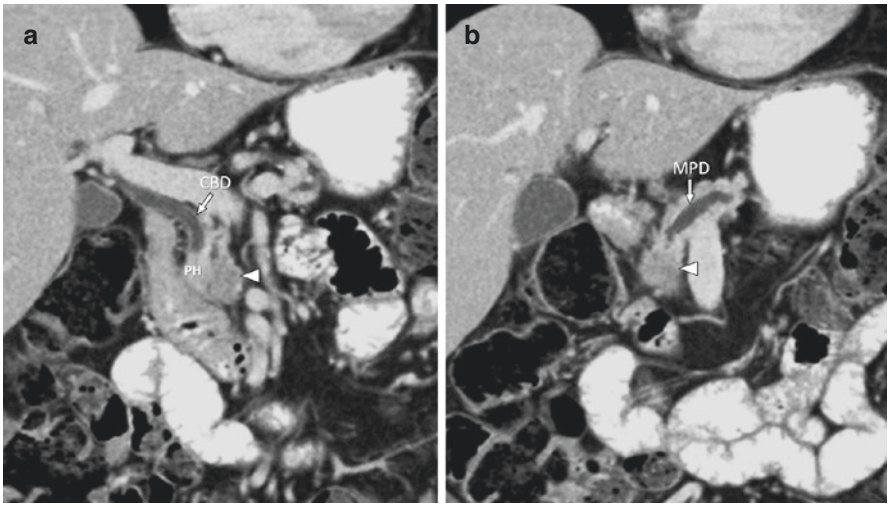

Fig. 15 Pancreatic adenocarcinoma, CT. Coronal reformations of a contrast-enhanced CT scan performed in a 70 year old woman with adenocarcinoma of the uncinate process of the pancreas. The lesion is again visualized as an area of reduced attenuation (arrowhead in Fig. a and b). Figure a shows how the lesion causes compression over the pancreatic head (PH) with biliary obstruction and retro-dilation of the common bile duct (CBD). Figure b shows retro-dilation of the main pancreatic duct (MPD), proximal to and extending immediately adjacent to the mass

5 Bowel

5.1 Appendicitis

Appendicitis is an inflammation of the vermiform appendix. It is a very common condition in general radiology practice and is one of the main causes for abdominal surgery in young patients. Clinical exam is key, but imaging may provide useful information for surgical decisions.

Acute appendicitis is most common between the ages of 10 and 20 years but may occur at any age, with a slight male predilection (male to female ratio of 1.4:1) [30].

The triggering factor in the development of acute appendicitis is the obstruction of the appendiceal lumen from any cause, commonly due to a fecalith (appendicolith).

Appendiceal luminal obstruction leads to distention, tissue ischemia, bacterial overgrowth, and inflammation. The inflammatory process can extend from the appendix to the adjacent peri-appendiceal fat and may also involve the cecum and terminal ileum.

The classical presentation of acute appendicitis consists of referred periumbilical pain, which within a day or later migrates to right iliac fossa, with associated loss of appetite, fever, nausea, and vomiting. However, not all patients present in a typical manner.

Imaging techniques for the evaluation of suspected appendicitis include plain radiographs and more commonly ultrasound and CT (Figs. 16 and 17).

Radiography has very low sensitivity and specificity for appendicitis. In perforated but contained appendicitis, the finding of free intraperitoneal air is infrequent because the inflammatory process is usually blocked off by the adjacent mesentery. Plain radiographs may show an appendicolith in a small number of cases. Rarely, dilated segments of small bowel may be recognized in the right lower quadrant as a result of obstruction from the inflammatory process (sentinel loop).

Ultrasound is recommended as an initial imaging study in children, thin young women, and pregnant women [31]. The sensitivity of US ranges between 44% and 98%, and its specificity ranges between 47% and 95% [32]. The primary ultrasound finding for the diagnosis of acute appendicitis is the presence of aperistaltic, non-compressible, blind-ended tubular structure with a diameter $\geq$ 6 mm cross section in the right iliac fossa with thickened wall (>3 mm) and a targetoid or laminated appearance. The inflamed appendix may demonstrate wall hyperemia on color Doppler ultrasound; an appendicolith may be identified as a rounded intraluminal calcified deposit with associated distal shadowing.

The fat surrounding the appendix may appear echogenic due to the inflammation and focal fluid collections or reactive enlarged lymph nodes may be present.

The sensitivity and specificity of CT examination of appendicitis range between 87% and 100% and 89% and 99%, respectively [32], and CT involves a relatively small dose of ionizing radiation.

CT features of acute appendicitis are comparable to US findings: a distended fluid-filled appendix with a thickened, hyperenhancing wall, peri-appendiceal fat

Fig. 16 Acute appendicitis, CT. Reformatted coronal intravenous contrast-enhanced CT image shows a thick walled, distended, fluid-filled appendix (arrow) with adjacent peri-appendiceal inflammatory stranding or dirty fat

stranding, and extraluminal fluid. An appendiceal diameter greater than 6 mm is indicative of appendicitis (Table 3).

A calcified appendicolith may be present in the appendiceal lumen. An indistinct wall or focal areas of absent enhancement may indicate ischemia and infarction, while signs of perforation include phlegmon, abscess, and extraluminal air [33].

The evolution of the inflammatory process can lead to appendicular perforation and consequent complications, which most commonly include abscess and peritonitis. Abscess is the most frequent complication of perforation [34]. CT shows a loculated, rim-enhancing fluid collection that may have mass effect on adjacent bowel loops (Figs. 18 and 19).

Bacterial peritonitis is a dangerous complication more common in young children, due to appendiceal rupture before formation of inflammatory adhesions.

CT and sonography can show between-loop fluid and free fluid following the peritoneal reflections, even far from the appendix. Frequent sites are the pelvis, the paracolic gutters, and the subhepatic and subphrenic spaces.

Uncommon complications include gangrenous appendicitis (CT findings of wall pneumatosis, shaggy appendiceal wall, and patchy areas of mural nonperfusion)

Fig. 17 Acute appendicitis, sagittal CT. Acute appendicitis shows a fluid-filled dilated appendix (arrow) with thickened wall, fat stranding and small amount of free fluid in the right paracolic gutter and in the Douglas pouch

Table 3 CT findings of appendicitis in symptomatic patients

CT findings	Interpretation
<6 mm appendix or >6-mm-thin walled appendix, completely gas-filled	Excludes appendicitis
6–10 mm appendix + wall thickening + wall hyperenhancement (no fat stranding)	Probable appendicitis
>10 mm appendix or >6 mm appendix + wall thickening + wall hyperenhancement + fat stranding	Definite appendicitis

and bowel obstruction secondary to entrapment of the distal ileum in a periappendiceal phlegmon.

Several alternative conditions may mimic appendicitis, and distinguishing between each is important because many are self-limited and respond to conservative treatment. Differential diagnosis include mesenteric adenitis, cecal diverticulitis, omental infarction, infectious terminal ileitis, IBD, perforated appendiceal carcinoma, and mucocele. *Yersinia enterocolitica* is the most common cause of mesenteric adenitis in North America, temperate Europe, and Australia.

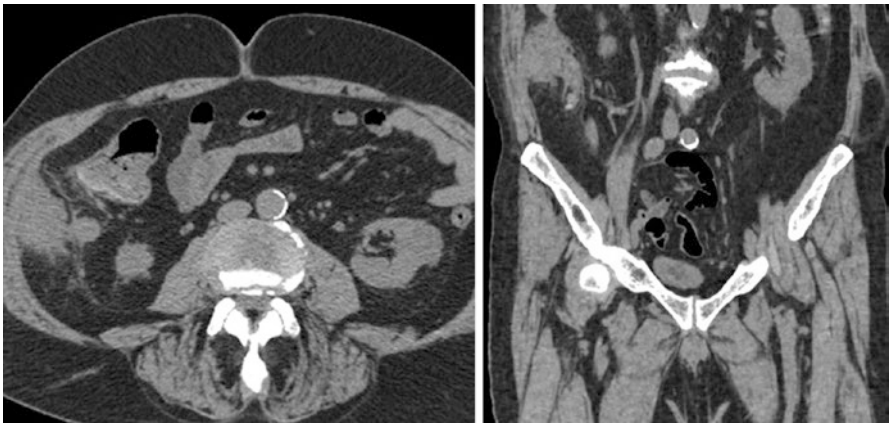

Fig. 18 Acute appendicitis with peri-appendiceal abscess, CT. Non-contrast axial and coronal CT scans show a fluid-filled blind-ending tubular structure on the right flank (arrow) with a subhepatic abscess (lateral arrow). The appendix is distended due to an obstructing hyperdense appendicolith (arrow, right image)

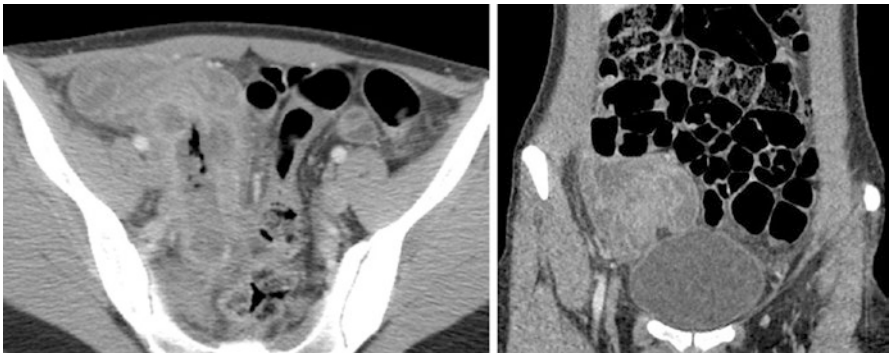

Fig. 19 Acute appendicitis with peri-appendiceal abscess, CT. Contrast-enhanced axial and coronal CT scan of an inhomogeneous fluid collection with enhancing rim, consistent with appendiceal abscess, within the right iliac fossa involving terminal ileum from a perforated appendix, confirmed by surgery

5.2 Diverticulitis

Diverticulosis (presence of diverticula) is a common condition in Western society, affecting 5–10% of the population over 45 years of age and approximately 80% of those over 85 years of age [35]. Diverticula can occur anywhere throughout the colon but are most common in the sigmoid colon. They represent acquired herniations of the mucosa and portions of the submucosa through the muscularis propria.

Diverticula occur mostly where the vessels penetrate the muscularis. Diverticula vary in size but usually range from 2–3 mm up to 2 cm.

Diverticular disease of the colon represents a continuum from an initial, pre-diverticular phase of marked muscular thickening of the colon wall, to frank outpouching (diverticulosis) and finally to frank diverticular inflammation (diverticulitis).

The clinical management of patients with acute diverticulitis depends on the severity, type, and extent of the pericolic inflammatory changes. For mild forms of diverticulitis, medical management with antibiotic therapy and supportive care is adequate.

Surgical resection is indicated for complicated forms, either at the time of the diagnosis or after an interval of antibiotic therapy and percutaneous abscess drainage [36]. Tube drainage of diverticular abscess may cool it down and allow for a single stage resection procedure (without a colostomy phase).

Approximately 15% of patients will require surgery for diverticular disease [37].

Complicated diverticulitis includes a broad spectrum of disease presentation, ranging from small pericolic abscesses to perforation with generalized peritonitis and sepsis, as well as late complications, including fistula and stricture formation.

The most commonly used grading system to describe the severity of complicated diverticulitis is the Hinchey classification (Table 4).

In most patients with acute diverticulitis, abdominal radiographs are of limited value and do not contribute to the diagnosis. Radiographs can be diagnostic only in the most severe forms of diverticulitis, in which the patient presents with free abdominal air.

CT is now considered the gold standard for assessing diverticulitis and its complications (Figs. 20, 21, and 22).

At CT, diverticulosis appears as small, air-filled outpouchings of the colonic wall, more numerous in the sigmoid colon. The wall of the involved colonic segment may appear thickened due to muscular hypertrophy.

In mild diverticulitis, the most frequent finding is a slight increase in the attenuation of fat adjacent to the involved colon, with engorgement of the vasa recta. The degree of fat stranding may vary from minimal "dirty fat" to severe inflammation. Dirty, inflamed fat appears as hyperattenuation relative to the hypoattenuation of normal fat on CT.

Fine linear strands, small fluid collections, and several bubbles of extraluminal air may be present. In more severe cases, pericolic heterogeneous fluid collections (phlegmons) or intramural/ extraintestinal abscess can occur. On CT, abscesses appear as fluid collections that may contain bubbles of air or air-fluid levels, with

Table 4 Classification of acute diverticulitis (Hinchey)

1a	Pericolic phlegmon and inflammation
1b	Diverticulitis with pericolic or mesenteric abscess
2	Diverticulitis with walled off pelvic abscess
3	Diverticulitis with generalized purulent peritonitis
4	Diverticulitis with generalized fecal peritonitis

Fig. 20 An example of uncomplicated diverticulitis, CT. Contrast-enhanced axial CT demonstrates edema and thickening of the sigmoid colon wall with multiple diverticular outpouchings (arrow) and fat stranding involving the sigmoid mesocolon around the diverticula, representing mild diverticulitis

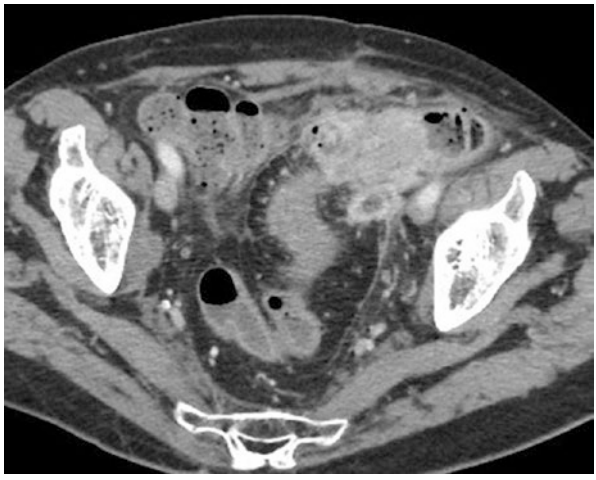

Fig. 21 Diverticulitis with confined peri-sigmoid inflammation, CT. Axial contrast-enhanced CT image shows diverticulitis with edematous sigmoid colon, multiple diverticula and perisigmoid abscess with enhancing wall (arrow) and fat stranding

central necrotic component and peripheral ring enhancement. These collections can appear near to the involved segment of the colon, or they can form at a distance: in the psoas muscle, flank, groin, thigh, subphrenic space, or liver. Other complications such as bowel obstruction, hepatic abscess, and fistula can often be demonstrated with CT. Fistulas frequently communicate with an abscess or other hollow viscus (more commonly the bladder). Severe complications necessitate intensive management. This is not to be confused with epiploic appendagitis, which can look like dirty fat benzene rings on CT in the pericolonic fat (from loss of blood flow to the small fatty appendages on the antimesenteric side of the colon, due to twisting or thrombosis in the small central draining vein).

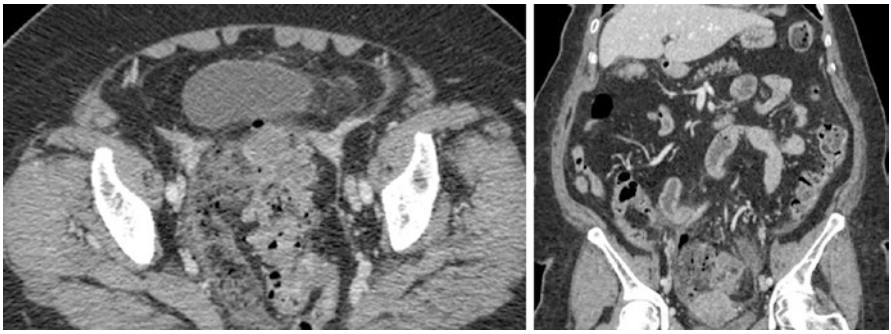

Fig. 22 Free perforation of sigmoid diverticulitis with the development of peritonitis, CT. Contrast-enhanced axial and coronal CT images of the sigmoid colon shows segmental mural thickening and multiple diverticula surrounded by inflammatory fat stranding and a perisigmoid abscess with free air bubbles. These findings suggest perforated diverticulitis and combined peritonitis, confirmed by surgery

5.3 Idiopathic Inflammatory Bowel Disease

Inflammatory bowel disease (IBD) is a chronic idiopathic disease affecting the gastrointestinal tract that include two related intestinal disorders, ulcerative colitis (UC) and Crohn's disease (CD). The etiology of IBD is still unknown; currently, the prevalent theory is an inappropriate immune response to gut luminal microbes in genetically susceptible people who are exposed to environmental risk factors. There is no gender predominance in IBD, with peak age of onset between 15 and 30 years of age but affecting people of all ages. Up to 20% of people with IBD are diagnosed during infancy, and the prevalence and incidence of pediatric IBD are growing worldwide [38].

5.3.1 Crohn's Disease

The pathologic findings in Crohn's disease are highly dependent on the duration of disease. Early disease presents superficial aphthoid ulcers of the mucosa that may become confluent. There is progression from limited mucosal disease to transmural inflammation of the bowel with collagen deposition eventually. Collagen deposition leads to obliteration of the submucosa, which results in stricture formation that may lead to obstruction.

Crohn's disease can involve any portion of the gastrointestinal tract from the mouth to the anus, although the small bowel is the most commonly affected portion of the bowel, particularly the RLQ distal and *terminal ileum* [39].

The earliest phases of small bowel inflammation may be characterized only by subtle mucosal hyperenhancement on the arterial phase images, with little or no wall thickening.

As the degree of inflammation progresses, the typical feature is bowel wall thickening of 1–2 cm. During the acute phase, the colon preserves mural stratification and often has a "target" or "double halo" appearance, due to submucosal edema among inner (mucosa) and outer (muscularis propria) rings of high attenuation [40].

In patients with long-standing Crohn's disease, mural stratification is lost, so that the affected bowel wall typically has a homogeneous attenuation on CT, suggestive of fibrosis or intramural deposition of fat.

Extraluminal, locoregional manifestations of Crohn's disease include fibro-fatty proliferation, the loss of the sharp interface between the involved bowel segment and mesentery, small mesenteric lymph nodes (from 3 to 8 mm), hypervascularization, and dilatation of the involved mesentery ("comb" sign).

CT evaluation may be useful to assess extraluminal disease complications of CD (e.g., fistula formation between bowel loops and between bowel and other visceral organs, abdominopelvic abscesses, or perforations) or extraintestinal manifestations of disease (e.g., renal lithiasis and sacroiliitis) [41] (Fig. 23). Air in the bladder in a young patient without bladder catheterization is from a fistula in Crohn's disease until proven otherwise.

Ultrasound findings of CD include mural wall thickening, loss of mural stratification, and increased blood flow at color Doppler imaging and often show that the colon has less peristalsis and less compressibility than normal.

5.3.2 Ulcerative Colitis

Ulcerative colitis is a diffuse inflammatory disease that primarily involves the colorectal mucosa but later extends to other layers of the bowel wall. The disease begins in the rectum and extends proximally in a continuous pattern to involve either part of the colon or its entirety.

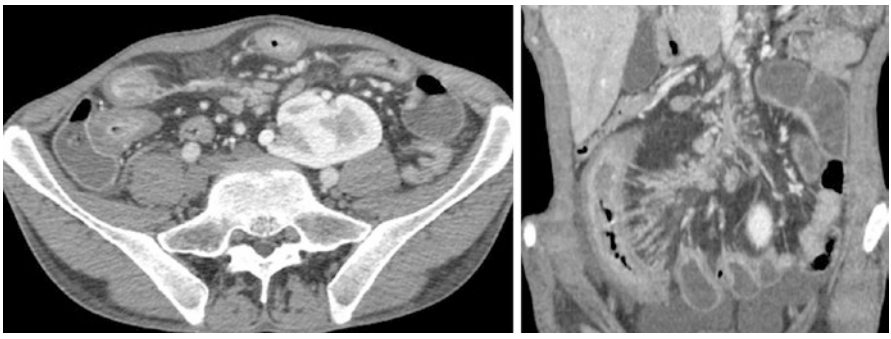

Fig. 23 Active Crohn's disease, CT. Contrast-enhanced axial and coronal CT images show marked wall thickening and hyperenhancement of the terminal ileum (arrow), near the ileocecal valve, with free peritoneal fluid and enlarged mesenterial lymph nodes. These findings suggest active inflammatory Crohn's disease, confirmed by endoscopy

Clinically, patients have chronic diarrhea, sometimes bloody, associated with tenesmus, pain, and fever. Some patients may have extraintestinal manifestations.

Abdominal X-rays can provide information in the acute setting, assessing for bowel perforation and toxic megacolon.

The radiological hallmark of active UC is the presence of colonic mural thickening and enhancement with luminal narrowing. A mean wall thickness of 8 mm has been reported in UC patients with active disease [42].

Radiological features of chronic UC may also include deposition of fat in the colonic wall, rectal narrowing, and consequent widening of presacral space and stranding of perirectal fat.

CT has an important role in the evaluation and detection of complications in patients with UC (Fig. 24). Toxic megacolon is a rare but very serious complication of UC. CT findings of toxic megacolon include luminal distension with thinning of the colonic wall and pneumatosis. Severe cases can lead to perforation and free air.

Beyond radiological imaging, colonoscopy is the principal modality for diagnosing and determining extent of disease in UC. In fact, mucosal abnormalities that characterize the early stages of the disease are beneath the spatial resolution of CT.

5.4 Small Bowel Obstruction

Small bowel obstruction (SBO) is a common clinical condition representing 20% of surgical admission for acute abdominal pain [43].

Since clinical findings are neither sensitive nor specific enough to determine the severity of SBO, the radiological investigation is fundamental in confirming the diagnosis, identifying its underlying cause, and detecting complications that require prompt surgery.

Plain abdominal radiography is the initial examination due to its wide availability and low cost (Fig. 25). However, radiographs are diagnostic in only 50–60% of cases and have high sensitivity only for high-grade obstruction [44].

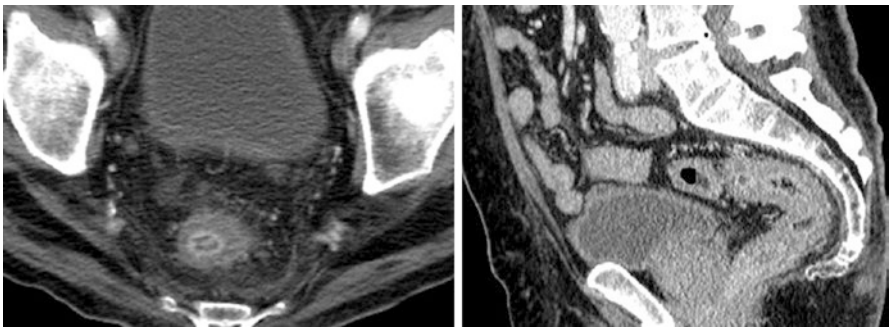

Fig. 24 Active ulcerative colitis, CT. Contrast-enhanced axial and sagittal CT scans show thickened rectal and sigmoid walls with target sign and inflammatory fat stranding (arrow). Active ulcerative colitis was confirmed by endoscopy

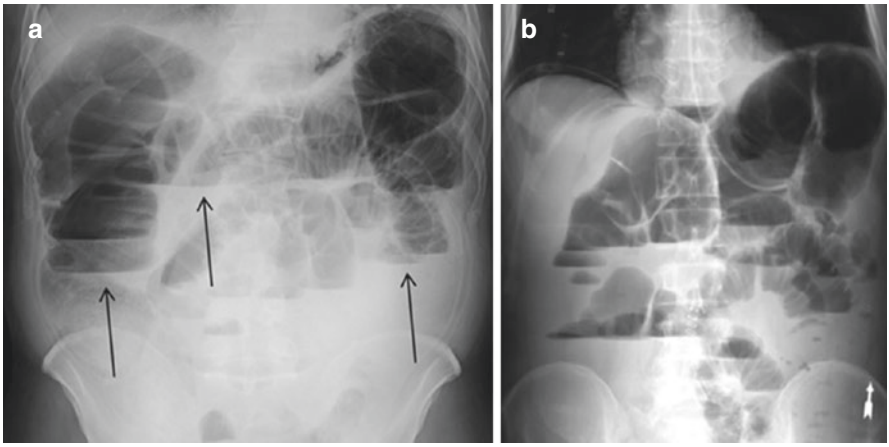

Fig. 25 High-grade SBO, Radiograph. Plain abdominal radiographs show multiple air-fluid levels within the small bowel. Active bowel peristalsis (**a**) working against the blockage results in air-fluid levels (black arrows) of varying heights in different locations (craniocaudal).In contrast, because of minimal peristalsis, an adynamic ileus (**b**) demonstrates air-fluid levels of the same or similar height (red and blue arrows). Radiograph *b* shows a paralityc ileus after abdominal surgery

Table 5 Diagnosis of SBO

Criteria	Specific criteria for diagnosis of SBO
Major	Small bowel dilated to 2.5 cm or greater and colon not dilated. Transition point from dilated to nondilated small bowel.
Minor	Air fluid levels. Colon decompressed.

The key radiographic signs of significant SBO is the presence of small bowel distention (greater than 3 cm), the absence of colonic dilatation, and the presence of multiple air-fluid levels (at different levels vs ileus which has air-fluid levels at the same horizontal level) (Table 5).

The cause of obstruction is generally not detectable on simple radiography.

US has a limited role in the assessment of SBO because of poor visualization of gas-filled structures.

CT is considered the best imaging modality for the assessment of bowel obstruction with a high accuracy. The typical features on CT include dilated proximal small bowel (>2.5 cm) with collapsed distal small bowel and colon. Air-fluid levels are also present [45].

In high-grade or chronic obstruction, the presence of particulate feculent material mixed with gas bubbles in the small bowel creates an appearance analogous to feces in the colon, the "small bowel feces" sign [46].

The main importance of this sign is that it is usually seen just proximal to the transition point (Fig. 26) [47].

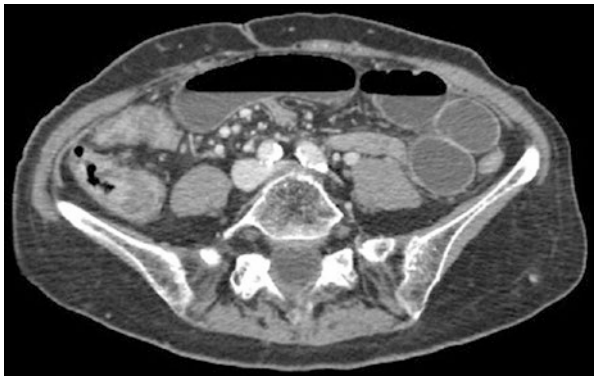

Fig. 26 Identification of the transition point in an SBO secondary to post-surgery adhesions, CT. Contrast-enhanced CT scan shows dilated small bowel loops. There is an abrupt change in caliber between the proximal dilated bowel loops and collapsed distal bowel loops. The change in caliber was due to adhesions

Fig. 27 SBO, CT. Small bowel feces sign in a patient with high-grade SBO secondary to postoperative adhesions. Contrast-enhanced oronal CT scan shows the presence of feculent material mingled with gas bubbles in the lumen of dilated loops of the small intestine. Small bowel can be identified with recognition of the valvulae conniventes (plica circulares, arrow)

Further, CT provides important information about the bowel wall, mesenteric vessels, and adjacent mesenteric fat, allowing the identification of coexistent ischemia or bowel perforation and free extraluminal gas (Fig. 27).

Causes of SBO can be divided into intrinsic to the bowel, extrinsic, and intraluminal. Adhesion is the most common cause of SBO, accounting for approximately 70% of all SBOs [48], but may show nothing on imaging, other than a transition point (Table 6).

Table 6 Causes of SBO

Causes of small bowel obstruction		
Intrinsic causes	Extrinsic causes	Intraluminal causes
Inflammatory diseases (Crohn's, tuberculosis, eosinophilic gastroenteritis) **Neoplasias** (primary or secondary) **Vascular lesions** (radiation enteropathy, ischemia) **Hematoma** **Intussusception**	**Adhesions** **Hernias** (external, internal) **Hematomas**	**Gallstones** **Bezoars** **Foreign bodies**

Approximately 80% of patients with SBO due to adhesions have a history of prior intra-abdominal surgery; the remainder have prior peritonitis or no precipitating causes.

Adhesions represent bands of fibrous tissue that obstruct the lumen, as a consequence of an inflammatory process. They are infrequently seen on CT, and the diagnosis is made by exclusion.

An abrupt change in the caliber of the small bowel with kinking or tethering at the transition zone, without any other identifiable cause, is highly suggestive of adhesion.

External hernias are the second most frequent cause of SBO [48]. They involve most frequently the inguinal canal or the anterior abdominal wall.

In cases of hernias, bowel obstruction occurs if there is incarceration (Fig. 28).

SBO due to hernia manifests with dilated bowel up to the hernia sac followed by decompressed bowel exiting from the sac. Internal hernias occur though acquired or congenital defects in the mesentery, through which bowel may traverse.

In patients with known primary tumors, the most likely cause of SBO is metastatic involvement of the bowel or the peritoneum, in the form of peritoneal carcinomatosis [49]. Tumors with a tendency to cause extensive diffuse peritoneal metastases include ovarian, colonic, pancreatic, and gastric neoplasms.

Primary neoplastic causes of SBO are rare. Intrinsic small bowel neoplasms constitute less than 2% of gastrointestinal malignancies, and they usually manifest at an advanced state as an irregular mural thickening at the transition point [50].

Malignancies that involve the cecum and colon can also result in SBO when there is involvement of the ileocecal valve.

SBO may occur in Crohn disease with an acute presentation or as the manifestation of a long-standing disease, which usually results in stenosis of affected segments.

Intussusception refers to telescoping of a proximal segment of the gastrointestinal tract within the lumen of the downstream segment. Adult intussusception represents 5% of all cases of intussusception and accounts for only 1–5% of intestinal obstructions in adults, whether idiopathic or secondary to any pathologic lesion of the bowel wall [51].

Fig. 28 SBO from incarcerated hernia, CT. Reformatted sagittal contrast-enhanced CT scan shows herniation of small bowel loops through an abdominal wall defect (arrow). The sac of the hernia contains extraluminal fluid and fluid-filled, mildly thickened bowel loops and causes SBO. Incarceration with small bowel obstruction was confirmed at surgery

The typical features of CT include a heterogeneous "target" shaped soft tissue mass with a layering effect; mesenteric vessels within the bowel lumen are also characteristic.

SBO is rarely caused by intraluminal material. The site of obstruction is usually at the ileocecal valve. Gallstone ileus is a mechanical obstruction due to impaction of one or more gallstones within the gastrointestinal tract that typically manifests with the Rigler triad, SBO, pneumobilia, and ectopic gallstone, usually in the right iliac fossa.

Closed-loop obstruction occurs when a segment of bowel is obstructed at two points along its course, resulting in progressive accumulation of fluid in gas within the isolated loop, placing it at risk for volvulus and subsequent ischemia.

Ischemia is the complication that increases the morbidity and mortality in patients who undergo surgery for SBO; when ischemia is suspected, immediate surgery is required to avoid transmural necrosis and perforation.

The CT findings of ischemia include bowel wall thickening, fluid in the adjacent mesentery, mesenteric edema, decreased bowel wall enhancement, and intestinal pneumatosis with or without associated mesenteric or portal venous gas [52].

5.5 Colorectal Cancer

Colorectal carcinoma (CRC) comprises approximately 90% of all large bowel tumors and is a major cause of morbidity and mortality in the western world. Worldwide, CRC is the third most commonly diagnosed cancer in both men and women. CRC incidence patterns are generally similar in men and women. The lifetime risk for developing colorectal cancer is 5–6% and increases with age; the typical age of diagnosis is during the sixth and seventh decades of life.

The CRC mortality has declined over the past two decades, due to advances in early detection and treatment [53]. The majority of CRC cases are sporadic (80%), and the rest are the result of genetic mutations [54]. The adenoma-carcinoma sequence accounts for approximately 70% of CRC pathogenesis, which takes 7–10 years to progress from benign adenoma to malignant tumor, which is why screening colonoscopy or virtual colonoscopy is typically recommended every 5 years. Sessile serrated polyps are associated with mutations and do not follow the usual rules of slow predictable transition from adenomas; therefore more frequent colonoscopy may be indicated.

The signs and symptoms of CRC vary and include abdominal pain, hematochezia, melena, unexplained iron deficiency anemia, diarrhea, obstruction, and bowel habit changes. However, there are no specific symptoms of early-stage colon cancer.

The initial diagnosis of CRC is usually made with colonoscopy. Colonoscopy allows biopsy samples to be taken for definitive diagnosis with a simultaneous opportunity for a therapeutic polypectomy.

Imaging, however, plays a fundamental role in determining the stage of disease at diagnosis.

In some cases, the radiologist may be the first to suggest the diagnosis of colon cancer in patients who undergo abdominal CT as the initial imaging modality for a variety of gastrointestinal symptoms.

The sensitivity of CT in detection of primary colon cancer is variable and depends on the size of the tumor [55].

The TNM classification is commonly used for staging of colorectal cancer and is based on the extent of tumoral, nodal, and metastatic involvement (Table 7).

On CT (Fig. 29), CRC commonly presents as asymmetric, short-segment wall thickening, or soft tissue mass that narrows the colonic lumen, with or without an irregular surface. Early-stage CRC can be seen as a polypoid or fungating mass without extracolonic tumor extension. Large tumors may appear as a mass with a central area of low attenuation due to necrosis.

Bulky fungating cancers most often arise in the cecum and ascending colon. Adenocarcinomas in the transverse and descending colon frequently become infiltrative and ulcerating, forming annular constricting tumors that narrow the lumen, referred to as eaten "apple-core" lesions.

Sometimes, it can be difficult to differentiate between benign and malignant colon wall thickening. Imaging features such as asymmetry, loss of haustral pattern, destruction of wall layer pattern, and "shouldered" edges favor malignant colon wall thickening. Classic boards case is iron deficiency anemia and a circumferential

Table 7 TNM staging colorectal adenocarcinoma

The AJCC TNM Staging (eighth Edition) classification for colon and rectal cancer	
Classification	Definition of TNM classification
Primary tumor (T)	Primary tumor cannot be assessed
TX	No evidence of primary tumor
T0	Carcinoma in situ
Tis	Tumor invades submucosa
T1	Tumor invades muscularis propria
T2	Tumor invades through muscularis propria into the pericolorectal tissues
T3	Tumor invades through the visceral peritoneum
T4	Tumor directly invades or adheres to other adjacent organs or structures
T4a	
T4b	
Lymph nodes (N)	Regional lymph nodes cannot be assessed
NX	No regional lymph node metastasis
N0	Metastasis in 1–3 regional lymph nodes
N1	Metastasis in four or more regional lymph nodes
N2	No distant metastasis by imaging
Distant metastasis (M)	Distant metastasis
M0	
M1	

Fig. 29 Cecal adenocarcinoma, CT. Axial contrast-enhanced CT scan show marked circumferential thickening of the cecum. Low-attenuation may represent fluid or necrosis. Adenocarcinoma was confirmed at endoscopy.

"apple-core" cancer lesion on barium enema or CT. Conversely, the presence of fluid in the root of the sigmoid mesentery and engorgement of adjacent sigmoid mesenteric vasculature favor the diagnosis of benign conditions, more often diverticulitis [56].

Owing to its ability to demonstrate the colon and surrounding structures, CT allows detection of regional extension of tumor. Extra-colic spread of tumor is demonstrated by thickening and infiltration of pericolic fat and loss of fat planes between the colon and adjacent organs [57]. Regional lymph node involvement may be seen.

The liver is the most common site of metastasis in patients with colorectal cancer due to its anatomical situation with regard to portal circulation [58]; thus, accurate imaging of the liver is essential.

Hepatic metastases can vary widely in size and usually appear as hypoattenuating masses, which are best visualized during the portal venous phase of liver enhancement. Liver metastases may be amenable to surgical resection, percutaneous thermal ablation, or radioembolization in interventional radiology/interventional oncology.

Other common sites of metastases from colon cancer include the lungs, adrenal glands, and bones.

CT is fundamental for postoperative surveillance for recurrence, both local and distant, and to document "normal" postoperative anatomy. Recurrent tumor after surgery usually appears as a soft tissue mass in or near the surgical anastomosis or in the liver.

CRC can be associated with diverse complications such as obstruction, intussusception, ischemia, perforation, and fistula formation with adjacent organs (Figs. 30 and 31).

Obstruction is the most common complication and is more frequent with left-sided colon cancers because of the smaller diameter of the left colon. The incidence rate of bowel obstruction associated with colon cancer is 8–29% [59]. Right-sided lesions more commonly present with bleeding and anemia, whereas left colon lesions often present with obstructive symptoms. Left may have a better prognosis than right CRC, and left is more likely to respond to the addition of an EGFR-targeted agent.

Perforation can occur either at the site of primary tumor, due to necrosis, or proximal portion of the tumor due to increased luminal pressure. Reported frequency of perforation and abscess formation associated with colon cancer is 2.5–10% and 0.3–4%, respectively [59].

Fig. 30 Cutaneous fistulization of colonic carcinoma in a patient with peritoneal carcinomatosis, CT. Contrast-enhanced axial CT scan shows widespread peritoneal metastases and free abdominal fluid with a colonic loop opened into an abscess and a fistula (arrow) communicating to the skin

Fig. 31 Colonic perforation in a patient with a history of sigmoid adenocarcinoma who presented with pain and sepsis, CT. Contrast-enhanced sagittal reformatted CT scan shows extensive extraluminal air and free fluid in the abdomen. Focal scleroses involve the lower lumbar and sacral vertebrae, consistent with blastic metastases. Note the metastatic bone involvement of the iliac wing in the axial scan. Surgery confirmed sigmoid cancer perforation.

5.6 Carcinoid Tumor

Carcinoid tumors are a type of neuroendocrine tumor typically found throughout the gastrointestinal tract, with distal predilection in the small bowel. A smaller percentage of them may involve other organs such as the lung, liver, ovary, and thymus. They are slow-growing tumors capable of metastasizing commonly to the mesentery, liver, and lymph nodes.

Clinical presentation of gastrointestinal tract carcinoid depends on the location. More often asymptomatic and usually found incidentally, they can sometimes present as abdominal pain, weight loss, fatigue, and diarrhea.

Chromogranin A is a valuable diagnostic biomarker since elevated serum values are associated with different types of neuroendocrine tumors. It may be found alone or in combination with a 5-hydroxyindoleacetic acid (5-HIAA) test, which suggests a functioning carcinoid tumor.

Carcinoid tumors involving the jejunum and ileum can be large at presentation. On CT, they appear as a well-defined hyperenhancing solid mass associated with desmoplastic reaction and retraction of adjacent small bowel loops. Central calcifications are often described, most frequently in the primary mesenteric masses [60].

5.7 Intestinal Vascular Disorders

5.7.1 Mesenteric Ischemia

Mesenteric ischemia is caused by reduced or interrupted splanchnic perfusion due to arterial or venous occlusion or hypotension. It may be acute or chronic.

Acute mesenteric ischemia (AMI) can be categorized into four specific types based on its cause: arterial embolism (most frequent cause of AMI, responsible for approximately half of cases), arterial thrombosis, nonocclusive mesenteric ischemia, and mesenteric venous thrombosis [61].

The final common pathway of all the specific causes of mesenteric ischemia is bowel infarction.

Clinical presentation is often nonspecific and in most cases can be characterized by a discrepancy between severe abdominal pain and minimal clinical findings. In general, patients with superior mesenteric artery (SMA) embolism or thrombosis have an acute onset of symptoms and a rapid deterioration in their clinical condition.

The mortality rate in patients with acute mesenteric ischemia exceeds 60% [62].

Chronic mesenteric ischemia accounts for less than 5% of intestinal ischemia. Atherosclerotic occlusion or severe stenosis is the most common cause. Symptoms occur when at least two of the three main splanchnic vessels (celiac trunk, superior mesenteric artery, or inferior mesenteric artery) are affected [63] (Fig. 32).

Abdominal radiographs are usually nondiagnostic in the setting of mesenteric ischemia and either are normal or show nonspecific signs.

Although historically, catheter angiography was the gold standard for imaging of suspected intestinal ischemia, CT/CTA is now the investigation of choice. CT allows the visualization of the mesenteric vasculature, bowel, and the entire abdomen for other processes.

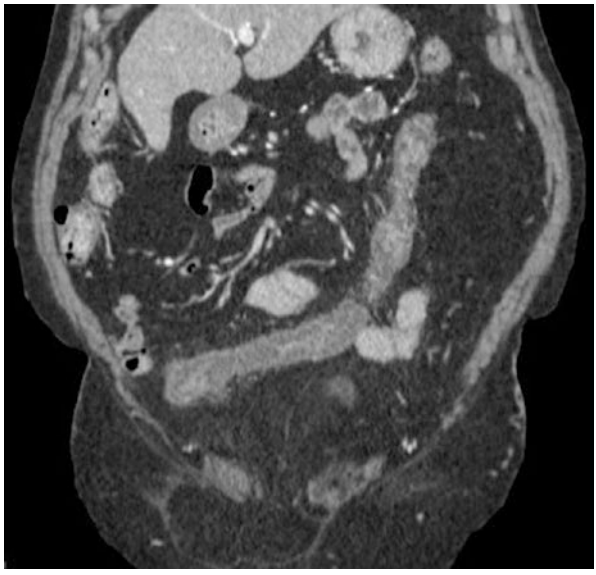

Fig. 32 Ischemic colitis, CT. Contrast-enhanced coronal CT scan shows fat stranding and wall thickening involving the transverse colon through the proximal left colon (arrow). Endoscopic findings confirmed the diagnosis of segmental ischemic colitis

The mesenteric vessels should be evaluated on unenhanced images for arterial calcifications and on intravenous contrast-enhanced CT images for the presence of thrombus or embolus. Acute arterial thrombi and emboli appear as low-attenuation filling defects in the SMA, its branches, or other major mesenteric arteries.

While large emboli and thrombosis may occlude the proximal SMA and major mesenteric vessels causing extensive small bowel and colon ischemia, smaller emboli can obstruct the distal portions of the vessel and lead to smaller regions of segmental ischemia [64]. Filling defects may have high attenuation in the vessels on non-enhanced CT images.

The bowel wall should be assessed on unenhanced images for the presence of increased attenuation, a specific sign of mural hemorrhage.

The presence or lack of contrast enhancement is evaluated on contrast-enhanced images. The absence of bowel wall enhancement is the most specific sign of acute mesenteric ischemia that suggests cessation of arterial flow. It usually indicates transmural infarction [65].

Pneumatosis intestinalis (the presence of gas within the wall of the gastrointestinal tract) is a typical finding of transmural bowel ischemia. The coexistence of pneumatosis intestinalis and porto-mesenteric gas has a very high specificity for ischemic bowel [66]. However, pneumatosis intestinalis is not a specific finding of intestinal ischemia and may occur in a wide range of benign conditions such as COPD or steroid use; however, when found, bowel ischemia must be first excluded [67].

In cases of venous occlusion, circumferential bowel wall thickening, typically under 1.5 cm, is the most common finding. The degree of wall thickening, however, does not correlate with the severity of mesenteric ischemia.

CT findings of venous ischemia include decreased mural enhancement, segmental mesenteric fat stranding, and free fluid interleaved between folds of the mesentery (Table 8).

Thrombosis within the mesenteric veins may appear as a low-attenuation filling defect on contrast-enhanced CT.

In cases of chronic mesenteric ischemia, the small bowel usually appears normal but may have a malabsorption pattern with fluid-filled loops, bowel wall thickening, and free peritoneal fluid. The diagnosis is supported by the presence of calcified atheromatous plaque at the origin of the mesenteric arteries and demonstration of arterial occlusions or severe stenoses in at least two of the three main splanchnic arteries.

5.7.2 Ischemic Colitis

Ischemic colitis refers to inflammation of the colon secondary to decrease in blood flow in the small arterioles of the colon. Most patients with colonic ischemia are elderly and present with mild lower abdominal pain and rectal bleeding. The clinical course and the outcome are highly variable.

Table 8 CT findings in intestinal ischemia

Features	Arterial ischemia	Venous ischemia	Nonocclusive ischemia
Incidence	60–70%	5–10%	20–30%
Acuity	Acute or chronic	Acute or chronic	Acute or chronic
Clinical risk factors	Cardiovascular disease. Septic emboli. Systemic vasculitis	Bowel strangulation, hypercoagulable state, portal hypertension, infection	Hypotension, heart failure, recent surgery or trauma, medications
Vasculature	Arterial filling defect, severe arterial narrowing, dissection, aneurysm	Venous filling defect	Nonspecific
Bowel wall thickness	Thin (acutely) or thickened; may be involved with hematoma, edema, or inflammation	Thickened and edematous	Generally thickened
Bowel wall enhancement	Variable	Diminished enhancement of mucosa and serosa, target appearance	Diminished enhancement
Mesentery/fat	Mesenteric fat stranding with free fluid associated with the territory of ischemia	Mesenteric fat stranding with free fluid associated with the territory of ischemia	Mesenteric fat stranding with free fluid associated with the territory of ischemia

The underlying pathophysiology of colonic ischemia is insufficient blood supply to the bowel with consequent injury. This leads to mucosal ulceration, inflammation, and hemorrhage. With disease progression, necrosis of the muscle layer can lead to the fibrotic stricture or transmural infarction.

Any portion of the colon and rectum can be affected, but the splenic flexure, descending colon, and sigmoid colon are the most involved segments. The splenic flexure is the most susceptible as a "watershed zone," furthest from the IMA and SMA interconnected flow (but supplied by the "arc of Riolan" and the more peripheral or outer "marginal artery of Drummond," which anastomose the IMA and SMA in the colon mesentery).

Most patients with colonic ischemia have no major vascular occlusion, so the condition is attributed to low blood flow states, small vessel disease, or sepsis.

CT and colonoscopy are the primary means of establishing the diagnosis of ischemic colitis.

The most common CT findings in ischemic colitis are bowel wall thickening, mesenteric fat stranding, and abnormal wall enhancement. The distribution of findings is segmental in most cases [68].

Pneumatosis coli and porto-mesenteric venous gas are infrequent but threatening findings of complicated ischemic colitis, together indicating transmural infarction.

6 Adrenal Glands

The adrenal glands are paired retroperitoneal endocrine organs, located above the upper poles of the kidneys. The adrenal glands usually display a linear, comma, and V or Y shape.

On ultrasound, the adrenal glands are studied at the same time as the kidneys. Low frequency allows more depth of penetration and deep images. In the adult, the glands are often not detectable on US unless enlarged.

CT is the primary modality for detection and characterization of adrenal masses [69]. Fatty thickening of adrenal tissue is usually adenoma. Fat has negative CT numbers on CT and has fatty characteristics on MRI as well (signal drop out with fat suppression sequences) also indicating adenoma.

6.1 Functioning Adrenal Masses

This category includes adrenal enlargement (hyperplasia) and adrenal masses (adenoma and pheochromocytoma).

Diffuse adrenal hyperplasia is a nonmalignant growth of the gland, seen on non-contrast CT scan as an enlarged adrenal gland with preserved morphology.

Functioning adrenal adenoma is the minority of adrenal adenomas. The non-contrast CT evaluation displays a hypodense mass characterized by attenuating values less than 10 HU due to fat contents. If it is unilateral, there may be atrophy of the contralateral gland [70].

Pheochromocytoma is an uncommon, more often sporadic adrenal tumor. It is called the "ten percent tumor" or "rule of tens" because in 10% of the cases it is malignant, 10% familial, 10% extra-adrenal, and 10% bilateral. In a non-contrast CT scan it appears as a large mass, sometimes with calcifications. After intravenous contrast media injection, it shows an early, strong, and inhomogeneous enhancement; the malignant form infiltrates contiguous structures and may develop hepatic metastases [69].

6.2 Nonfunctioning Adrenal Masses

Nonfunctioning adrenal masses include benign (hematoma and adenoma) and malignant lesions (carcinoma).

Hematoma can result from traumatic or nontraumatic causes. On non-contrast CT, hematoma appears as hyperdense circular mass (acute phase) or with pseudocystic "water-like" density (chronic phase). After contrast media, no enhancement is observed.

Nonfunctioning adenoma is generally detected incidentally (incidentaloma). It appears as a well-circumscribed, hypodense formation (−10/+20 HU) with possible outbreaks of cystic degeneration and calcifications. After contrast, enhancement is appreciated in the parenchymal phase and strong washout in the late phase [69].

Carcinomas are rare non-secreting malignant tumors that occur as large masses with calcifications in 35% of cases. In CT after contrast medium administration, they show inhomogeneous enhancement due to areas of necrosis [70]. Survival is improved with aggressive application of surgical resection and local percutaneous thermal ablation therapy.

7 Kidneys

The ultrasound examination is the first level of examination in the study of the urogenital system and can identify hydronephrosis or stone disease.

CT has a relevant role in the diagnosis of urothelial obstruction, neoplasm, trauma, and vascular pathology [71].

The administration of intravenous contrast medium shows the whole excretory system with different phases: cortico-medullary (25–40 s postinjection) with bright outer kidney, nephrographic (80–100 s) with equally enhanced cortex and medulla, and excretory (~3–10 min) when the renal collecting system is opacified and full.

7.1 Renal Stones

The first level exams are abdomen X-ray or KUB (kidneys, ureter, and bladder) and ultrasound. X-ray is useful primarily to identify radiopaque stones. Ultrasound reveals radiopaque and radiolucent kidney stones that appear as hyperechoic nodules with a posterior shadow or cone. Renal ultrasound can easily detect dilation of the proximal collecting system, but evaluation of the lumbar and pelvic segments of the ureter is limited (even when very dilated) by bowel gas obscuration. Air is no friend of US; think why dolphins can speak over miles of waterways, since sound waves travel best in water. This is also why US is so good at differentiating between cystic and solid structures.

CT is the gold standard in the study of nephrolithiasis: the stones are characterized by high attenuation values (Fig. 33) [71].

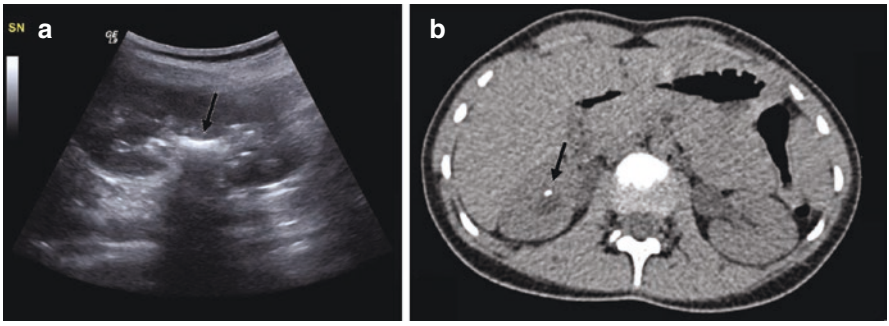

Fig. 33 Kidney stones. (**a**) At US, kidney stones are hyperechoic structures (arrow) with posterior shadow cone. (**b**) Non-contrast CT-scan is the gold standard in the study of renal lithiasis: the stones are characterized by high attenuation values (arrow)

The use of the contrast medium is indicated in the case of failed or uncertain identification of stones, in the suspicion of other obstructive pathology (clots, neoplasms), suspected complications (pyelonephritis, abscesses), or treatment planning.

7.2 Pyelonephritis

Acute pyelonephritis is generally of bacterial origin. At ultrasound, the edematous kidney is large and hyperechoic. On contrast-enhanced CT, pyelonephritis occurs as a non-enhancing hypodense focal area. Diffuse pyelonephritis manifests as an enlarged and hypodense kidney due to interstitial edema. Contrast administration shows lack of cortico-medullary differentiation and delay of the nephrographic phase (Fig. 34) [71].

Chronic pyelonephritis on CT is characterized by a small kidney, often associated with compensatory hypertrophy of the contralateral kidney. With contrast, thinning of the renal cortex, deformed calva calyxes, and a compensatory columnar hypertrophy can be identified [71].

7.3 Kidney Infarction

Occlusion of the renal artery or its branches may be total or regional/district.

In the acute phase, total infarction of the kidney appears hypodense due to edema without parenchymal enhancement or excretion of contrast media. It may be associated with subcapsular fluid collections and reactive thickening of the fascial planes.

In regional infarction during the nephrographic phase, a wedge-shaped hypodense area may be apparent with a cortical base and apex toward the renal hilum. Chronic renal infarction may show a small non-enhancing kidney (total infarction) or hypodense cuneiform foci with cortical retraction (district or regional infarction).

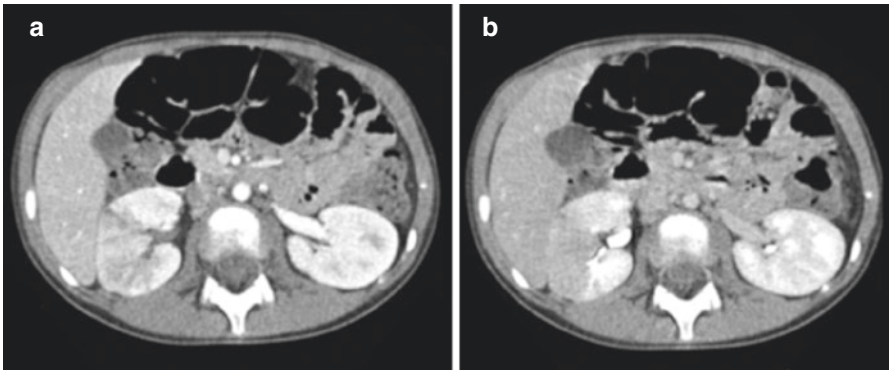

Fig. 34 Pyelonephritis, CT. Pyelonephritis manifests as a hypodense focal area: no enhancement after contrast medium injection is seen. Contrast medium administration shows the lack of cortico-medullary differentiation (**a**) and delay of the nephrographic (**b**)

7.4 Renal Masses

In most cases, renal masses are incidentally detected during abdominal imaging performed for other reasons.

At ultrasound, two types of kidney lesions, cystic or solid, can be recognized and should be characterized by a CT scan if previously unknown [71].

In general, renal masses fall into three categories by their appearance on contrast-enhanced CT: those without enhancement, those with enhancement, and those with macroscopic fat [71].

7.4.1 Cysts

Cysts are fluid-filled masses of varying dimensions characterized by thin and sharp epithelial wall.

At ultrasound, cysts are anechoic with posterior acoustic enhancement, although this may not be seen with smaller cysts (Fig. 35).

On a non-contrast CT scan, uncomplicated cysts are uniformly hypodense (less than 20 HU), the wall is not visible, and its attenuation value does not increase after intravenous contrast media injection (less than 10 HU).

Cysts are complicated, if the CT attenuation values increase after contrast media administration or if they have thickened septa or calcification [71].

Complicated cysts could result from infection or intracystic hemorrhage, but in most cases, they are identical to cystic tumors. The Bosniak classification has been created to assess the likelihood of malignancy in cysts and differentiate between benign and potentially malignant cystic lesions.

7.4.2 Angiomyolipoma

Angiomyolipoma (AML) is the most common benign solid renal mass, and it is made up of fat, vessels, and atypical muscle fibers.

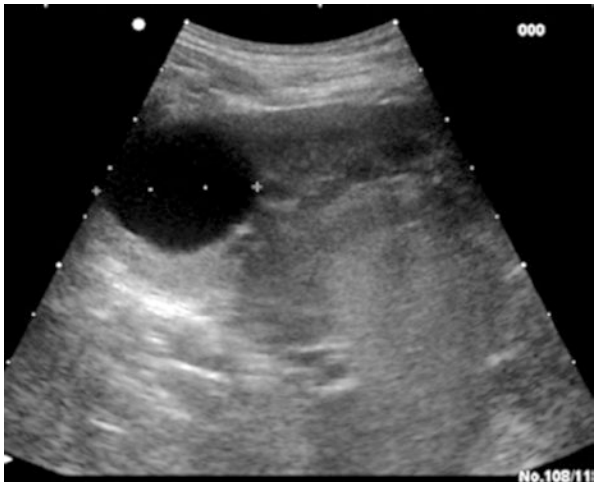

Fig. 35 Renal Cyst, US. Cysts in most cases are incidental findings during ultrasound examinations performed for other reasons. Cysts are anechoic (arrow) with posterior acoustic enhancement (arrows) but this finding may not be evident with smaller cysts

At ultrasound, AMLs are hyperechoic relative to renal parenchyma and often an incidental finding in asymptomatic patients (Fig. 36) [72], unless they present with bleeding or pain.

If the hyperechoic lesion is small (<3 cm), the diagnosis of AML is more likely [72].

The detection of fat (attenuation values less than −20 HU) on a CT scan confirms the diagnosis of AML. Rarely (5%) AMLs do not contain macroscopic fat, and these lesions are indistinguishable from RCC on CT. If calcifications and fat are detected in the same lesion, the diagnosis of renal cell carcinoma is more probable [71, 72]. AML >4 cm diameter may require prophylactic embolization due to bleeding risk, and the presence of pseudoaneurysms >5 mm further implies risk for subsequent spontaneous bleeding, which can be induced by trauma. Fatty masses ("lipo") will shrink less over time than more solid or vascular masses ("angio + myo") following embolization. Repeated embolizations may be required over time, depending upon growth rates, symptoms, and risk.

7.4.3 Oncocytoma

Oncocytoma is the second most common benign solid renal mass.

On US, it appears like an iso-hypoechoic solid lesion with well-defined margins.

On CT, oncocytomas are characterized by uniform contrast enhancement indistinguishable from a renal cell carcinoma or other malignant tumor (Fig. 37). Sometimes in larger lesions, a central scar may be detectable, which is a characteristic of oncocytomas, but it is seen only in a third of cases.

7.4.4 Renal Cell Carcinoma

Renal cell carcinoma (RCC) is the most common adult renal epithelial cancer representing more than 85% of all renal malignancies. Imaging plays a significant role in the early diagnosis of this tumor before clinical signs are observed (macroscopic hematuria, flank pain, palpable flank mass) [72].

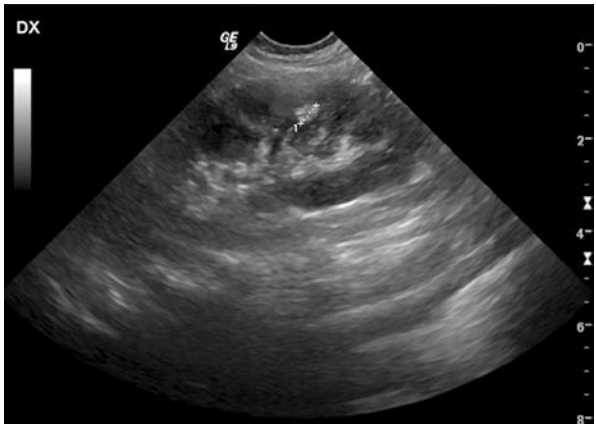

Fig. 36 Angiomyolipoma, US. On ultrasound, angiomyolipomas are hyperechoic to renal parenchyma (arrow) and often incidental finding in asymptomatic patients. If the hyperechogenicities are small (<3 cm), the diagnosis of AML is more probable

Fig. 37 Oncocytoma, CT. On contrast CT, oncocytomas are characterized by uniform enhancement (arrow) similar to renal cell carcinoma or other malignant tumor. Occasionally in the large lesions, a central scar may be detectable

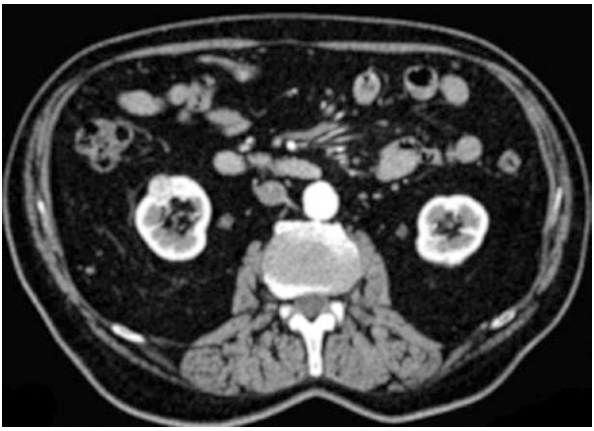

Fig. 38 Renal Cell Carcinoma, CT. On contrast-enhanced CT, renal cell carcinoma has strong enhancement (arrow) in the early arterial phase (corticomedullary phase) due to its hypervascularity

At ultrasound examination, it is a solid lesion, with irregular margins and varying sonographic appearance.

On non-contrast CT scan, RCC appears as inhomogeneous solid mass, with blurred margins, and in larger lesions, hypodense areas of necrosis can be present. Approximately 30% of cases demonstrate some calcifications [72].

After contrast media administration, RCCs strongly enhance in the early arterial phase (cortico-medullary phase). The parenchymal (nephrographic) phase is the most sensitive phase for the detection of RCC: the lesion is hypoattenuating to the normal parenchyma which has a homogeneous marked enhancement (Fig. 38) [72]. Hereditary RCC is seen with Von Hippel-Lindau disease which is associated with cerebellar hemangioblastomas and multiple RCC over a lifetime. About 5–10% of RCC are bilateral. RCC typically grow slowly at a rate of under 5 mm per year. They rarely metastasize when under 3 cm diameter. Under 3 cm diameter may be removed by partial nephrectomy or percutaneous ablation with RFA, microwave, or cryoablation in interventional radiology or interventional oncology. Interventional

radiology is the newest independent clinical residency in the USA, and IR has clinics, has admission privileges, and takes longitudinal care of patients, often as part of a multidisciplinary team. See chapter on minimally invasive image guided therapy ("video-game surgery").

References

1. Tom WW, Yeh BM, Cheng JC, Qayyum A, Joe B, Coakley FV. Hepatic pseudotumor due to nodular fatty sparing: the diagnostic role of opposed-phase MRI. AJR Am J Roentgenol. 2004;183(3):721–4.
2. Tchelepi H, Ralls PW, Radin R, Grant E. Sonography of diffuse liver disease. J Ultrasound Med. 2002;21(9):1023–32; quiz 33-4.
3. Hamer OW, Aguirre DA, Casola G, Lavine JE, Woenckhaus M, Sirlin CB. Fatty liver: imaging patterns and pitfalls. Radiographics. 2006;26(6):1637–53.
4. Kodama Y, Ng CS, Wu TT, Ayers GD, Curley SA, Abdalla EK, et al. Comparison of CT methods for determining the fat content of the liver. AJR Am J Roentgenol. 2007;188(5):1307–12.
5. Sirlin CB, Reeder SB. Magnetic resonance imaging quantification of liver iron. Magn Reson Imaging Clin N Am. 2010;18(3):359–81, ix.
6. Murakami T, Nakamura H, Hori S, Nakanishi K, Mitani T, Tsuda K, et al. CT and MRI of siderotic regenerating nodules in hepatic cirrhosis. J Comput Assist Tomogr. 1992;16(4):578–82.
7. Joshi G, Crawford KA, Hanna TN, Herr KD, Dahiya N, Menias CO. US of right upper quadrant pain in the emergency department: diagnosing beyond gallbladder and biliary disease. Radiographics. 2018;38(3):766–93.
8. Heller MT, Tublin ME. The role of ultrasonography in the evaluation of diffuse liver disease. Radiol Clin N Am. 2014;52(6):1163–75.
9. Kurtz AB, Rubin CS, Cooper HS, Nisenbaum HL, Cole-Beuglet C, Medoff J, et al. Ultrasound findings in hepatitis. Radiology. 1980;136(3):717–23.
10. Lee S, Kim DY. Non-invasive diagnosis of hepatitis B virus-related cirrhosis. World J Gastroenterol. 2014;20(2):445–59.
11. Gonzalez-Guindalini FD, Botelho MP, Harmath CB, Sandrasegaran K, Miller FH, Salem R, et al. Assessment of liver tumor response to therapy: role of quantitative imaging. Radiographics. 2013;33(6):1781–800.
12. Choi BI, Lee KH, Han JK, Lee JM. Hepatic arterioportal shunts: dynamic CT and MR features. Korean J Radiol. 2002;3(1):1–15.
13. Pesapane F, Nezami N, Patella F, Geschwind JF. New concepts in embolotherapy of HCC. Med Oncol. 2017;34(4):58.
14. Bruix J, Sherman M. Practice guidelines committee AAftSoLD. Management of hepatocellular carcinoma. Hepatology. 2005;42(5):1208–36.
15. Mathieu D, Vasile N, Fagniez PL, Segui S, Grably D, Larde D. Dynamic CT features of hepatic abscesses. Radiology. 1985;154(3):749–52.
16. Graves JA, Hanna TN, Herr KD. Pearls and pitfalls of hepatobiliary and splenic trauma: what every trauma radiologist needs to know. Emerg Radiol. 2017;24(5):557–68.
17. Boscak AR, Al-Hawary M, Ramsburgh SR. Best cases from the AFIP: Adenomyomatosis of the gallbladder. Radiographics. 2006;26(3):941–6.
18. Bortoff GA, Chen MY, Ott DJ, Wolfman NT, Routh WD. Gallbladder stones: imaging and intervention. Radiographics. 2000;20(3):751–66.
19. Brink JA, Simeone JF, Mueller PR, Saini S, Tung GA, Spell NO, et al. Routine sonographic techniques fail to quantify gallstone size and number: a retrospective study of 111 surgically proved cases. AJR Am J Roentgenol. 1989;153(3):503–6.
20. Smith EA, Dillman JR, Elsayes KM, Menias CO, Bude RO. Cross-sectional imaging of acute and chronic gallbladder inflammatory disease. AJR Am J Roentgenol. 2009;192(1):188–96.

21. Grand D, Horton KM, Fishman EK. CT of the gallbladder: spectrum of disease. AJR Am J Roentgenol. 2004;183(1):163–70.
22. Chung YE, Kim MJ, Park YN, Choi JY, Pyo JY, Kim YC, et al. Varying appearances of cholangiocarcinoma: radiologic-pathologic correlation. Radiographics. 2009;29(3):683–700.
23. Caremani M, Occhini U, Caremani A, Tacconi D, Lapini L, Accorsi A, et al. Focal splenic lesions: US findings. J Ultrasound. 2013;16(2):65–74.
24. Unal E, Onur MR, Akpinar E, Ahmadov J, Karcaaltincaba M, Ozmen MN, et al. Imaging findings of splenic emergencies: a pictorial review. Insights Imaging. 2016;7(2):215–22.
25. Lee HJ, Kim JW, Hong JH, Kim GS, Shin SS, Heo SH, et al. Cross-sectional imaging of splenic lesions: RadioGraphics fundamentals | online presentation. Radiographics. 2018;38(2):435–6.
26. Foster BR, Jensen KK, Bakis G, Shaaban AM, Coakley FV. Revised Atlanta classification for acute pancreatitis: a pictorial essay. Radiographics. 2016;36(3):675–87.
27. Busireddy KK, AlObaidy M, Ramalho M, Kalubowila J, Baodong L, Santagostino I, et al. Pancreatitis-imaging approach. World J Gastrointest Pathophysiol. 2014;5(3):252–70.
28. Sahani DV, Kambadakone A, Macari M, Takahashi N, Chari S, Fernandez-del CC. Diagnosis and management of cystic pancreatic lesions. AJR Am J Roentgenol. 2013;200(2):343–54.
29. Zins M, Matos C, Cassinotto C. Pancreatic adenocarcinoma staging in the era of preoperative chemotherapy and radiation therapy. Radiology. 2018;287(2):374–90.
30. Humes D, Speake WJ, Simpson J. Appendicitis. BMJ Clin Evid. 2007;2007
31. Mostbeck G, Adam EJ, Nielsen MB, Claudon M, Clevert D, Nicolau C, et al. How to diagnose acute appendicitis: ultrasound first. Insights Imaging. 2016;7(2):255–63.
32. Hernanz-Schulman M. CT and US in the diagnosis of appendicitis: an argument for CT. Radiology. 2010;255(1):3–7.
33. Pinto Leite N, Pereira JM, Cunha R, Pinto P, Sirlin C. CT evaluation of appendicitis and its complications: imaging techniques and key diagnostic findings. AJR Am J Roentgenol. 2005;185(2):406–17.
34. Hopkins KL, Patrick LE, Ball TI. Imaging findings of perforative appendicitis: a pictorial review. Pediatr Radiol. 2001;31(3):173–9.
35. Ferzoco LB, Raptopoulos V, Silen W. Acute diverticulitis. N Engl J Med. 1998;338(21):1521–6.
36. Feingold D, Steele SR, Lee S, Kaiser A, Boushey R, Buie WD, et al. Practice parameters for the treatment of sigmoid diverticulitis. Dis Colon Rectum. 2014;57(3):284–94.
37. Morris AM, Regenbogen SE, Hardiman KM, Hendren S. Sigmoid diverticulitis: a systematic review. JAMA. 2014;311(3):287–97.
38. Gasparetto M, Guariso G. Highlights in IBD epidemiology and its natural history in the Paediatric age. Gastroenterol Res Pract. 2013;2013:829040.
39. Zalis M, Singh AK. Imaging of inflammatory bowel disease: CT and MR. Dig Dis. 2004;22(1):56–62.
40. Raman SP, Horton KM, Fishman EK. Computed tomography of Crohn's disease: the role of three dimensional technique. World J Radiol. 2013;5(5):193–201.
41. Kilcoyne A, Kaplan JL, Gee MS. Inflammatory bowel disease imaging: current practice and future directions. World J Gastroenterol. 2016;22(3):917–32.
42. Jacobs JE, Birnbaum BA. CT of inflammatory disease of the colon. Semin Ultrasound CT MR. 1995;16(2):91–101.
43. Foster NM, McGory ML, Zingmond DS, Ko CY. Small bowel obstruction: a population-based appraisal. J Am Coll Surg. 2006;203(2):170–6.
44. Lappas JC, Reyes BL, Maglinte DD. Abdominal radiography findings in small-bowel obstruction: relevance to triage for additional diagnostic imaging. AJR Am J Roentgenol. 2001;176(1):167–74.
45. Mullan CP, Siewert B, Eisenberg RL. Small bowel obstruction. AJR Am J Roentgenol. 2012;198(2):W105–17.
46. Mayo-Smith WW, Wittenberg J, Bennett GL, Gervais DA, Gazelle GS, Mueller PR. The CT small bowel faeces sign: description and clinical significance. Clin Radiol. 1995;50(11):765–7.
47. Lazarus DE, Slywotsky C, Bennett GL, Megibow AJ, Macari M. Frequency and relevance of the "small-bowel feces" sign on CT in patients with small-bowel obstruction. AJR Am J Roentgenol. 2004;183(5):1361–6.

48. Miller G, Boman J, Shrier I, Gordon PH. Etiology of small bowel obstruction. Am J Surg. 2000;180(1):33–6.
49. Idelevich E, Kashtan H, Mavor E, Brenner B. Small bowel obstruction caused by secondary tumors. Surg Oncol. 2006;15(1):29–32.
50. Qalbani A, Paushter D, Dachman AH. Multidetector row CT of small bowel obstruction. Radiol Clin N Am. 2007;45(3):499–512, viii.
51. Marinis A, Yiallourou A, Samanides L, Dafnios N, Anastasopoulos G, Vassiliou I, et al. Intussusception of the bowel in adults: a review. World J Gastroenterol. 2009;15(4):407–11.
52. Paulson EK, Thompson WM. Review of small-bowel obstruction: the diagnosis and when to worry. Radiology. 2015;275(2):332–42.
53. Ward E, Sherman RL, Henley SJ, Jemal A, Siegel DA, Feuer EJ, et al. Featuring Cancer in men and women ages 20-49. J Natl Cancer Inst. 1999-2015;2019
54. Gollub MJ, Schwartz LH, Akhurst T. Update on colorectal cancer imaging. Radiol Clin N Am. 2007;45(1):85–118.
55. Dighe S, Purkayastha S, Swift I, Tekkis PP, Darzi A, A'Hern R, et al. Diagnostic precision of CT in local staging of colon cancers: a meta-analysis. Clin Radiol. 2010;65(9):708–19.
56. Horton KM, Abrams RA, Fishman EK. Spiral CT of colon cancer: imaging features and role in management. Radiographics. 2000;20(2):419–30.
57. So JS, Cheong C, Oh SY, Lee JH, Kim YB, Suh KW. Accuracy of preoperative local staging of primary colorectal Cancer by using computed tomography: reappraisal based on data collected at a highly organized Cancer center. Ann Coloproctol. 2017;33(5):192–6.
58. Sheth KR, Clary BM. Management of hepatic metastases from colorectal cancer. Clin Colon Rectal Surg. 2005;18(3):215–23.
59. Kim SW, Shin HC, Kim IY, Kim YT, Kim CJ. CT findings of colonic complications associated with colon cancer. Korean J Radiol. 2010;11(2):211–21.
60. Levy AD, Sobin LH. From the archives of the AFIP: gastrointestinal carcinoids: imaging features with clinicopathologic comparison. Radiographics. 2007;27(1):237–57.
61. Oldenburg WA, Lau LL, Rodenberg TJ, Edmonds HJ, Burger CD. Acute mesenteric ischemia: a clinical review. Arch Intern Med. 2004;164(10):1054–62.
62. Yasuhara H. Acute mesenteric ischemia: the challenge of gastroenterology. Surg Today. 2005;35(3):185–95.
63. Herbert GS, Steele SR. Acute and chronic mesenteric ischemia. Surg Clin North Am. 2007;87(5):1115–34. ix
64. Kirkpatrick ID, Kroeker MA, Greenberg HM. Biphasic CT with mesenteric CT angiography in the evaluation of acute mesenteric ischemia: initial experience. Radiology. 2003;229(1):91–8.
65. Kanasaki S, Furukawa A, Fumoto K, Hamanaka Y, Ota S, Hirose T, et al. Acute mesenteric ischemia: multidetector CT findings and endovascular management. Radiographics. 2018;38(3):945–61.
66. Dhatt HS, Behr SC, Miracle A, Wang ZJ, Yeh BM. Radiological evaluation of bowel ischemia. Radiol Clin N Am. 2015;53(6):1241–54.
67. Sebastià C, Quiroga S, Espin E, Boyé R, Alvarez-Castells A, Armengol M. Portomesenteric vein gas: pathologic mechanisms, CT findings, and prognosis. Radiographics. 2000;20(5):1213–24. discussion 24-6
68. Cruz C, Abujudeh HH, Nazarian RM, Thrall JH. Ischemic colitis: spectrum of CT findings, sites of involvement and severity. Emerg Radiol. 2015;22(4):357–65.
69. Wang F, Liu J, Zhang R, Bai Y, Li C, Li B, et al. CT and MRI of adrenal gland pathologies. Quant Imaging Med Surg. 2018;8(8):853–75.
70. Herr K, Muglia VF, Koff WJ, Westphalen AC. Imaging of the adrenal gland lesions. Radiol Bras. 2014;47(4):228–39.
71. Heilbrun ME, Remer EM, Casalino DD, Beland MD, Bishoff JT, Blaufox MD, et al. ACR Appropriateness Criteria indeterminate renal mass. J Am Coll Radiol. 2015;12(4):333–41.
72. Siegel CL, Middleton WD, Teefey SA, McClennan BL. Angiomyolipoma and renal cell carcinoma: US differentiation. Radiology. 1996;198(3):789–93.